Case Studies in Construction Materials 20 (2024) e02994

Contents lists available at ScienceDirect

Case Studies in Construction Materials

journal homepage: www.elsevier.com/locate/cscm

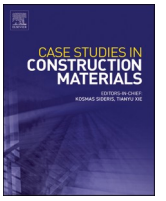

Case study

Mechanical performance of aged cement-based matrices reinforced with recycled aramid textile nonwoven fabric: Comparison with other FRCMs

Payam Sadrolodabaee [a,1], Albert de la Fuente [a,1], Mònica Ardanuy [b,*], Josep Claramunt [c,1]

[a] Department of Civil and Environmental Engineering, Universitat Politecnica de Catalunya (UPC), Jordi Girona 1-3, Barcelona 08034, Spain
[b] Department of Materials Science and Engineering, Universitat Politecnica de Catalunya (UPC), Colom 1, Terrassa 08222 Spain
[c] Department of Agri-Food Engineering and Biotechnology, Universitat Politecnica de Catalunya (UPC), Esteve Terradas 8, Castelldefels 08860, Spain

ARTICLE INFO

Keywords:
Accelerated aging
Cementitious composites
Flexural/tensile properties
Recycled fibers
Textile-reinforced mortars
Waste valorization

ABSTRACT

Utilizing recycled fibers as reinforcement in cement-based matrices is an effective means of promoting waste recycling and adopting a circular economy approach in the construction industry. Within this framework, the recycling and potential reutilization of textile residues can improve the pre- and post-cracking performance of cement-based matrices intended for building components with up to intermediate structural responsibilities (i.e., panels and cladding elements for buildings). This research is focused on the mechanical and durability -through forced aging of dry-wet and freeze-thaw cycles- experimental characterization of laminated fabric-reinforced cementitious matrices (FRCMs) containing 4 and 6 nonwoven fabric layers obtained from end-of-life fire-protecting t-shirts. For this purpose, both direct and flexural tensile tests were conducted to characterize the mechanical performance of the composite. The tests on the 6-fabric layers produced panels with Portland Cement (PC) matrix, after 28-day of curing, led to average values of the maximum tensile strength of 3.7 MPa with associated toughness index superior to 25 kJ/m^2, and mean modulus of rupture of 11.6 MPa with a fracture energy index of 4.3 kJ/m^2. After dry-wet accelerated aging, the post-cracking performance of the developed composites decreased (on average, 40% in toughness and 11% in strength) due to fiber embrittlement. To better understand the performance of aged composites, shredded fibers recovered from protective clothing (mainly consisting of meta-aramid fibers) were immersed in the binary matrix. Accordingly, the mechanical properties of the fibers after 5 and 10 cycles of dry-wet aging were studied. Based on the results, replacing partially PC by silica fume (between 30% and 50%) was seen as a sustainable alternative to improve the performance of the aged fibers by more than 10%.

* Corresponding author.
E-mail addresses: payam.sadrolodabaee@upc.edu (P. Sadrolodabaee), albert.de.la.fuente@upc.edu (A. de la Fuente), monica.ardanuy@upc.edu (M. Ardanuy), josep.claramunt@upc.edu (J. Claramunt).
[1] Co-authors.

https://doi.org/10.1016/j.cscm.2024.e02994
Received 11 December 2023; Received in revised form 29 January 2024; Accepted 18 February 2024
Available online 20 February 2024

1. Introduction

The building industry has the capacity (and challenge) to support in accomplishing sustainable development objectives and combating climate change since this industry accounts for more than 35% of carbon footprint, energy consumption, and waste generation [1]. To this end, it is essential to shift from the existing linear economic model to a circular economy approach emphasizing materials reuse and recycling [2]. Following this approach within the construction cycle, it is feasible to provide end-of-life components with a second life, either as aggregates [3–5], mineral additions [6], or reinforcements [7,8].

During the last decades, there has been a growing interest in the research on fiber-reinforced cementitious (FRC) materials due to their benefits (i.e., cracking control, increasing the material's energy absorption and tensile/flexural resistance) [9]. In this context, using short fibers derived from various natural or synthetic sources as reinforcement of cement-based composites has been extensively studied [10]. Among non-natural fibers, aramid fibers have emerged as a promising reinforcement option due to their excellent tensile strength and modulus, low density (up to 5 times higher strength/weight ratio than steel), as well as resistance to elevated temperatures and chemical degradation [11]. Several researchers have investigated the use of this fiber as an effective means to address the inherent brittleness and cracking tendency of cement-based composites. Among those, Morón et al. [12] reinforced recycled aggregate cement mortars with a 1% volume fraction (V_f) of 20 mm p-aramid fibers (Kevlar), reporting that the incorporation of dispersed aramid fibers improved the ultimate flexural resistance of plain recycled mortars by 10% while it had a negligible effect on the compressive strength. Further, the reinforced mortar showed up to 16% higher Modulus of Rupture (MOR) than the plain mortar (PM) after being subjected to the 25 freeze-thaw (FT) cycles. In another study, Curosu et al. [13] developed high-strength strain-hardening cementitious composites (SHCC) reinforced with temperature-resistant short p-aramid fibers (6 mm length and 12 μm diameter) by V_f of 2%. The results showed poor workability in aramid fiber-reinforced mortars in comparison to other composites (i.e., those reinforced with high-density polyethylene and high-modulus PBO fibers); however, the tensile performance of aramid composite, including first crack strength, also known as Bend Over Point (BOP), and Ultimate Tensile Strength (UTS) of 6.3 MPa and 9.4 MPa, respectively, as well as the compressive strength (f_c) of 144.8 MPa, were superior. Nonetheless, studies on incorporating recycled aramid fibers derived from textile wastes (TW) in cementitious composites are still scarce. Tran et al. [14] examined the incorporation of recycled aramid fibers in PM and concluded that the mix design optimized with short 12 mm length fibers in a V_f of 0.3% could enhance several design-sensitive properties (i.e., compressive and flexural strengths and shrinkage) by showing strain-softening behavior, especially in the case of recycled p-aramid. In another research [15], it was reported that hybrid recycled TW fibers from Kevlar/Nomex (blend ratio of 1:1) with V_f of 0.3% enhances the mechanical properties (f_c by 4.8% and MOR by 12%) of PM, while no significant effect was observed on the drying shrinkage.

Apart from the short randomly distributed fibers, reinforcing the cementitious matrices with non-metallic textile structures is considered a feasible way to attain high-strength and lightweight composites [16]. This type of material, well-known as fabric-reinforced cementitious matrix (FRCM) or textile-reinforced mortar (TRM) -the former being used for homogeneity hereinafter, has gained increasing interest among researchers and practitioners for retrofitting or as a stand-alone lightweight, thin-walled element for structural/non-structural applications [17,18]. The fabrics differ in geometry, distribution, and fiber types. The commercially available textile reinforcements are typical woven/knitted open meshes or crossed yarn systems made up of high-strength synthetic textiles, including carbon [19], alkali-resistance (AR) glass [20], basalt [21], PBO or aramid [22] (fewer studies available on the latter). On the other hand, natural-based textiles have been recently promoted due to sustainability awareness. Generally, the textiles (either synthetic or vegetal) are composed of several yarns, and the yarns are composed of filaments. Proper matrix penetration within the fabric and the filaments is required in any type of FRCM. As only the external filaments (sleeve) may be in direct contact (anchored) with the matrix, the polymer or resin coating could be fully or partially applied over the textile to bind all the filaments (both sleeve and core), this leading to better filament anchorage with more uniform stress distribution [23,24]. Further, it was reported that this technique could reduce the deterioration of both vegetal and synthetic fibers in the matrix's high alkalinity [25,26], as well as enhance the bond strength in the fabric-matrix interface by favoring tensile failure of the reinforcing textile rather than the textile slippage [27]. Nonetheless, it should be noted that using this coating treatment on natural-based fibers will negatively impact both the economic and environmental performances of this solution. For this reason, several authors have recently reported using mineral impregnation (e.g., nano-silica fillers) or graphene nanocomposite instead of polymers to overcome the challenges including sustainability, degradation at elevated temperatures, and limitation in drapability [28,29].

Nonwoven textile fabrics produced from vegetal or recycled fibers are seen as another promising sustainable reinforcement in FRCMs, mainly oriented for non-structural applications [30]. Porous and thin nonwoven fabrics could be produced with minimal labor requirements at a low cost from randomly distributed irregular fibers (short or long) entangled together through mechanical, chemical, or thermal processes [31]. Matrix penetrability into the nonwoven fabric mainly depends on the fabric's structure and fabrication technique, both optimized in previous research [32,33]. Based on those results, the optimum fabric should have a 1–2 mm thickness and an areal weight between 140 and 250 g/m^2. In nonwoven FRCM systems, the fabric is entirely immersed into the matrix and coated with the paste. Thus, fabric-to-matrix interlocking is distinct from the woven systems constituting internal and external filaments, which may cause textile slippage (telescopic failure). In previous works [34–36], laminated FRCMs with 100% flax and hybrid nonwoven (65% recycled fashion textile waste fibers + 35% flax fibers) were produced. Those findings suggested that hybrid textile waste (HTW) composite could be a viable replacement for those counterparts composed of 100% vegetal fibers since the durability and sustainability characteristics were improved [37,38]. Indeed, recovering/recycling fibers from readily available waste sources, such as textile residues, could promote the circular economy model and reduce the costs and environmental impact of waste dumping [39]. The textile industry, as the fourth main contributor to greenhouse gas emissions and resource use, produces million tons of waste worldwide (e.g., more than ten million tons in Europe yearly), including both pre-consumer and post-consumer waste [40,41]. These

Table 1
Data Summary of the uniaxial tensile properties of woven synthetic and vegetal FRCMs.

Textile type (V_f or W_f if reported)	Textile properties		Matrix type (fc in MPa if reported)	Tensile test set-up of composites		Composite properties					REF
	T_s [MPa]	E_s [GPa]		Coupon size [mm]	Gripping system	UTS [MPa]	BOP [MPa]	E_1 [GPa]	ε_u [%]	Failure mode	
Uni-directional dense aramid	1265	137	PC mortar with short fibers; (10.0)	500 × 100 × 10	Mechanical clamping with steel tabs; gage length of 340 mm	1089 (per textile area); 25.0* (per composite area)	170 (per textile area); 3.9* (per composite area)	108 (per textile area)	1.9	A	[22]
Quadriaxial aramid	758	60				1354 (per textile area); 49.5* (per composite area)	596 (per textile area); 21.8* (per composite area)	1446 (per textile area)	1.6	B	
Bi-directional coated aramid–glass (warp direction)	1829	101.5	Polymer-modified PC mortar; (22.8)	600 × 50 × 10	Hydraulic clamping with FRP sheets	1875 (per textile area)	761 (per textile area)	404 (per textile area)	1.7	C	[45]
100% aramid warp-knitted (V_f =1.3%)	2370	55	Plain PC paste; (51.0)	250× 30× 9	Hydraulic clamping with metal tabs; gage length of 150 mm	25.9	1.0	16.0	2.5	B	[44]
100% PP warp-knitted (V_f =3.1%)	500	6.9				11.7	1.5	8.3	2.3	B	
Hybrid aramid-PP (50−50) warp-knitted (V_f =2.1%)	2370 and 500	55 and 6.9				14.8	0.7	23.1	2.8	B	
100% AR glass warp-knitted (V_f =2.3%)	1372	72				6.6	1.3	2.5	1.2	C	
100% aramid warp-knitted (V_f=1.9%)	2367	55	Plain PC paste	250× 34× 8	Clamping grip with metal tabs	26.2	3.0*	N.A.	4.3	D	[46]
100% PP warp-knitted (V_f=6.2%)	223	7				9.25	1.0*	N.A.	8	D	
Hybrid aramid-PP (50−50) warp-knitted (V_f=2.6%)	2367 and 223	55 and 7				25.75	4.0*	N.A.	4.1	D	
100% AR glass warp-knitted (V_f =1.1%)	1591	78				18.11	1.5*	N.A.	1.5	C	
100% AR-glass coated bi-directional woven - 4 layers (V_f =1.85%)	1046	N.A	77% PC+ 13% FA+ 10% SF; (104.0)	500× 60 × 10	Clamping grip with aluminum tabs	12.0	5.2	N.A.	0.8	C	[47]
100% E-glass coated bi-directional woven −4 layers (V_f =1.1%)	1121	N.A	77% PC+ 13% FA+ 10% SF; (104.0)			12.3	5.0	N.A.	1.1	C	
Uni-directional glass - 1 layer	2900	71	NHL+ pozzolan+ carbonate filler; (15.0)	300 × 60 × 8	Clamping grip with metal tabs	5.5	1.8*	3.9	0.8	C	[48]
Bi-directional sisal woven −3 layers (V_f=4.7%)	249	4.4				10.6	1.8*	4.2	7.9	D	
Bi-directional flax woven −3 layers (V_f=4%)	292	3.8				12.8	2*	4.3	12.0	D	
Uni-directional long-aligned sisal (V_f=10%)	400	19	50% PC+ 30% MK+ 20% calcined waste clay brick	400× 50 × 12	Hydraulic clamping with aluminum tabs; gage length of 200 mm	12.0	4.8	9.4	1.53	D	[49]
Bi-directional jute woven −5 layers	67	4.8	50% CEM II + 40% MK + 10% FA	450× 40 × 12	Clamping grip with steel tabs	4.73	2.31	N.A.	3.1	N.A.	[23]

(*continued on next page*)

Table 1 (*continued*)

Textile type (V_f or W_f if reported)	Textile properties		Matrix type (fc in MPa if reported)	Tensile test set-up of composites		Composite properties						REF
	T_s [MPa]	E_s [GPa]		Coupon size [mm]	Gripping system	UTS [MPa]	BOP [MPa]	E_1 [GPa]		ε_u [%]	Failure mode	
Coated bi-directional jute woven −5 layers	81	3.9				6.94	1.86		N.A.	6.6	N.A.	
Bi-directional flax - 2 layers	331	12.5	NHL (9.5)	500× 60 × ~8	Clevis grip with aluminum tabs; gage length of 300 mm	4.6	1.0	N.A.		6.3	C	[50]
Coated bi-directional flax - 2 layers	266	12.4				4.4	0.7		N.A.	5.1	C	
Coated woven hemp - 2 layers	173.3	11.6	Cement based mortar (39.2)	400× 50 × ~20	Clevis grip with steel plates; gage length of 200 mm	134.0 (per textile area); 5.3* (per composite area)	3.27	5.1		2.3	A	[24]
Coated woven sisal - 2 layers	137.2	4.9				127.5 (per textile area); 5.1* (per composite area)	2.78		6.4	2.7	C	

Notes: V_f or W_f: volume/weight fraction of fiber; T_s: tensile strength of textile; E_s: elastic modulus of textile; fc: compressive strength of the matrix; PC: Portland cement; FA: fly ash; SF: silica fume; NHL: natural hydraulic lime; MK: metakaolin; UTS: ultimate tensile stress of composite; BOP: bend over point as cracking strength of matrix; E_1: elastic modulus of the uncracked stage of composite; ε_u: failure strain capacity of composite; N.A.: Not available; *: estimated by us.

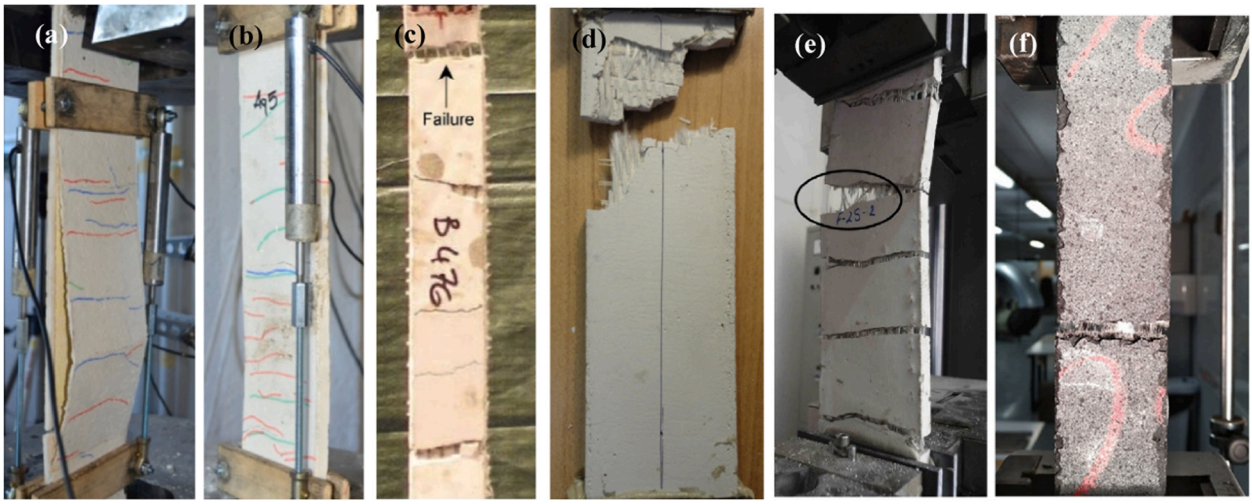

Fig. 1. Tensile failure modes of FRCMs: a) Matrix separation of aramid composite; b) Textile slippage of aramid composite; c) Tensile rupture of the aramid-glass composite; d) Tensile rupture of the glass composite; e) Fiber pull-out of flax woven composite; f) Fiber pull-out of flax-textile waste nonwoven composite (adapted from [22,34,45,48]).

end-of-life textile products, recycled and reused less than 18% [42], could be valorized as internal reinforcement of cementitious composites.

To further boost the circular economy, in this experimental study, new nonwoven fabrics produced from 100% recycled fibers derived from fire-protecting garments of firefighters (mainly consisting of meta-aramid fibers) were incorporated into PC matrices with reinforcement purposes. The performance of this multilayer FRCM was evaluated in unaged, dry-wet (DW) and freeze-thaw (FT) aged conditions through direct and flexural tensile tests. The obtained results from direct tension and 4-point bending tests were compared with their counterparts, mainly other nonwoven or vegetal woven fabrics, to adopt in real-life potential applications in construction. Further, the durability (through dry-wet accelerated aging) of these new short shredded recycled fibers immersed inside the PC matrix with various silica fume (SF) dosages was investigated, and accordingly, the tensile properties of the short fibers were evaluated. So far, a similar comprehensive experimental program on meta-aramid fibers recovered from used clothes as reinforcement in FRCMs is unavailable. Moreover, despite a few available comparative studies on the direct tensile performance of synthetic FRCMs [43], no comprehensive research compares the flexural and tensile behaviors of natural-based woven FRCMs with nonwoven ones. The outcomes and conclusions of this experimental research may pave the research on FRCM systems, specifically those containing recycled textile fibers.

2. A brief review of recent studies on FRCMs

To determine the realistic applications for the developed nonwoven FRCMs in the present study, the tensile and flexural design parameters of the typical FRCMs, including woven synthetic (aramid, polypropylene, glass) and plant-based (vegetable), obtained from several experimental programs reported in the literature, were listed in Table 1. While synthetic textile composites are mainly oriented for structural applications (retrofitting masonry/concrete elements), vegetable ones are seen as suitable for applications with low-to-medium structural responsibility (e.g., cladding panels, roofing tiles, pavements, strengthening of weak historical substrates, etc.). In this so-called sustainable type of FRCM with vegetal textiles, which generally have lower modulus/strength than those reinforced with synthetic fibers, the improvement of the composite toughness and ductility is the priority over the resistance. Indeed, the high-stiffness/resistance textiles may be unsuitable for some flexural-oriented applications as the load transfer mechanism to the stiff fibers may limit the resistant load capacity due to premature cracking or slippage [29,44]. Thus, low-stiffness and more sustainable (i.e., affordable and eco-friendly) textiles are promoted mainly for flexural-based non-structural applications.

Failure modes (Fig. 1): A: Matrix separation and debonding; B: Cracking of the matrix and textile slippage (mainly in the anchored zones); C: Tensile rupture of the textile (mainly in the central zone of the gauge length); D: Crack widening and Fiber pull-out.

As can be observed in Table 1, the thickness of the tested FRCM specimens was 10 ± 2 mm, except for one study with 20 mm. Based on recommendations [17,55], thicknesses below 6 mm and superior to 30 mm should be avoided in direct tensile test. The width and length of the specimens gathered in Table 1 ranged between 30 and 100 mm and 250–600 mm, respectively. Likewise, according to the RILEM TC-232 recommendation [55], the length-to-width ratio of the specimens in the tensile test should be at least 5. The method to guarantee the adequate gripping of the end coupons (clevis articulation or hydraulic/mechanical clamping) and strain measurement (LVTDs, potentiometers, extensometer, digital image correlation, or machine crosshead) are described in [43,56]. It should be noted that the gripping system may affect the general tensile behavior, including stress distribution and failure mode [43]. As reported by John et al. [57], unrestricted rotations in all principal directions were permitted by the clevis grip to avoid the parasitic bending

Table 2
Data Summary of the flexural properties of woven synthetic and vegetal FRCMs.

Textile type (V_f or W_f if reported)	Textile properties		Matrix type (fc in MPa if reported)	Flexural test set-up of composites			Composite properties					REF
	T_s [MPa]	E_s [GPa]		3PB/ 4PB	Coupon size [mm]	Span length [mm]	MOR [MPa]	LOP [MPa]	I_{GF} [kJ/ m^2]	D_u [mm]	ε_F [%]	
100% aramid warp-knitted (V_f =1.3%)	2370	55	Plain PC paste; (51.0)	3PB	250×30×9	220	46.9	5.9	15.1*	23.0	4.4*	[44]
100% PP warp-knitted (V_f =3.1%)	500	6.9					12.2	3.0	7.7*	32.9	6.1*	
Hybrid aramid-PP (50−50) warp-knitted (V_f =2.1%)	2370 and 500	55 and 6.9					44.3	5.1	20.3*	29.6	5.5*	
100% AR glass warp-knitted (V_f =2.3%)	1372	72					17.0	2.3	1.8*	14.0	2.7*	
Bi-directional AR glass - 2 layers	875	65.9	30% PC+ 50% FA + 5% SF+15% LS (37.0)	4PB	410× 90 × 20	300	13.0	5.4	4.6*	8.0	2.5*	[51]
Uni-directional long-aligned sisal −5 layers (V_f=10%)	400	19	50% PC + 30% MK + 20% calcined waste clay brick	4PB	400× 50 × 12	300	25.1	9.3	22.1	30.0	5.6*	[49]
Bi-directional flax woven (W_f=3.2%)	294.4	10.6	CEM II/B-M (39.1)	3PB	160× 40 × 40	100	6.5	5.6	7.8*	N.A.	N.A.	[52]
			CEM II/B-M +30% MK (49.1)				12.3	7.6	15.1*	N.A	N.A.	
Uni-directional long-aligned sisal- 5 layers (V_f=10%)	557	19	50%PC + 30% MK + 20% calcined waste clay brick (65.0)	4PB	400× 100× 12	300	17.8	6.2	21.7	50.0	9.4*	[53]
			100% PC				19.3	5.3	22.5	50.0	9.4*	

Notes: LS: limestone filler; 3PB or 4PB: 3 or 4-point bending tests; MOR: Modulus of Rupture; LOP: Limit of Proportionality as cracking strength of matrix; I_{GF}: flexural toughness or energy absorption index; Du: failure deflection capacity; ε_F: failure flexural strain capacity calculated based on ASTM D6272–17 [54]; N.A.: Not available; *: estimated by us.

derived from possible imperfections of the specimens. The clamping set-up was the most frequently used; nonetheless, a higher scatter of the failure modes (for the same textile type) was observed in contrast with the clevis set-up, as also concluded in [43].

Regarding synthetic FRCMs, composites reinforced with p-aramid textiles could obtain UTS higher than 25 MPa with a strain capacity (ε_u) of more than 2%. Authors of RILEM TC-250-CSM [22] investigated FRCMs considering uni-directional and quadriaxial dried aramid textiles, reporting that the latter composite had higher strength and stiffness but lower deformability. De Santis et al. [45] studied the tensile behavior of a cement composite reinforced by coated fabric from glass and aramid yarns in the warp direction and of only glass yarns in the weft direction. In [22] and [45], the tensile stress of FRCMs was expressed as the ratio of the measured load to the cross-sectional area of the textile (not the whole composite specimens) in order to eliminate the effect of the mortar thickness variability. Nonetheless, based on the provided data in the first study, the tensile stress per composite gross cross-section was considered, aiming to compare consistently with the results derived from other studies. The differences in tensile strength and Young's modulus between the two calculation methods were clearly significant.

Mobasher et al. [44] compared the mechanical behavior of pultruded cement boards reinforced with four layers of warp-knitted fabrics made of 100% aramid, 100% polypropylene (PP), hybrid textiles from 50% aramid–50% PP, and 100% AR glass. Based on the results, the 100% AR glass FRCM proved the lowest resistance (UTS = 6.5 MPa) and strain ($\varepsilon_u = 1.2\%$) compared to other fabrics. Similarly, Peled et al. [46] developed pultruded cement composites reinforced with three layers of fabrics from the same yarns. However, in this research, the 100% PP fabric showed the least tensile resistance (9.2 MPa), almost half of the 100% AR glass. Paul and Gettu [47] recently compared FRCM reinforced with AR and coated E-glass textiles in self-compacting matrices, both reaching UTS > 12 MPa. After examining the durability performance of developed FRCMs through aging in hot water immersion, the authors concluded that E-glass FRCM with appropriate coating could be a cost-efficient alternative to AR-glass textiles.

With the purpose of investigating FRCMs with enhanced sustainability performance, Cevallos et al. [48] produced composites reinforced with three layers of woven natural-based fabrics (flax and sisal) through the hand lay-up molding technique. The authors compared the results of vegetal FRCMs with the counterpart produced with one layer of glass textile. Although the properties of the glass textile (tensile strength and modulus) were one order of magnitude higher than the vegetal fabrics, both UTS and ε_u of the vegetal FRCMs were significantly higher than those reported for the glass FRCM (at least 2 and 8 times, respectively). Further, the glass FRCMs in all previous studies ([44,46,48]) had a rather brittle failure mode (i.e., tensile rupture of the textile in the gauge length) with both low deflection and strain at failure. Indeed, textiles with a high modulus of elasticity (like glass) may fail more frequently under textile rupture mode rather than pull-out, which is more dominant in the case of vegetal FRCMs.

Within also the context of vegetal FRCMs, Silva et al. [49] produced five layer-laminated panels from long uni-directional aligned sisal fibers (400 mm), reaching UTS of 12 MPa (similar to that achieved in the composites presented in [48]). Fidelis et al. [23] experimentally characterized the tensile behavior of the composites reinforced with five layers of the jute fabric, both uncoated and coated with the polymer styrene-butadiene, in a low calcium hydroxide (CH) matrix. The composite containing treated fabrics (impregnated for 50 minutes in the polymer) led to the highest crack number and smaller spacing, reaching UTS of 7 MPa with a ε_u of 7%. Ferrara et al. [50] investigated the tensile behavior of uncoated and polymer-coated flax FRCMs (one and two layers) in a hydraulic-lime mortar matrix. The authors concluded that the coating strategy adopted, although causing a beneficial effect on the tensile behavior of composite (especially with one layer of textile), led to significant variability of the results and diminished the sustainability performance of the vegetal FRCMs. In another recent study on the FRCMs with epoxy resin-coated vegetal fabrics (hemp and sisal) [24], UTS > 5 MPa (per cross-sectional area of the specimen) with limited strain capacity ($\varepsilon_u < 3\%$) were obtained.

Research on the flexural performance of FRCMs (Table 2) is scarce compared to the studies reporting on direct tensile performance. Mobasher et al. [44] studied the flexural performance of the previously mentioned FRCMs and reported that the composites of aramid textiles had three times higher MOR than those reinforced with only PP and AR glass. AR-glass FRCMs in quaternary blended cements with only 30% PC were recently developed by Alma'aitah and Giassi [51,58] achieving MOR higher than 13 MPa. The authors reported that when the matrix was reinforced with 2% short AR-glass or PVA fibers, the MOR and strain capacity of the developed composites reached 20 MPa and 3.5%, respectively. As for sustainable vegetal FRCMs, Silva et al. [49] presented experimental tests in which up to 25 MPa of MOR with five layers of long-aligned sisal textile, with notable toughness (22 kJ/m^2), were reached. Majstorovi'c et al. [52] developed FRCM composites reinforced with 12 layers of flax woven fabric in PC and binary systems matrices (Metakaoline by 30%). These authors reported, unlike other studies [53,59–61], that the substitution of supplementary cementitious materials (SCMs) could increase the 28-day strength of both the matrix and the composite in comparison to PC samples, and by doing so, reaching MOR of 12 MPa in the tested composites. Toledo Filho et al. [53] could produce a sisal FRCM with a MOR of 19 MPa and a deflection as high as 50 mm.

Thus, according to the gathered data on the tensile and flexural mechanical properties of various woven FRCMs (p-aramid, PP, glass and vegetal), the following can be concluded:

- A wide range of mechanical results and heterogeneity of failure modes for specific textile reinforcement have been observed, making the comparison exercise non-conclusive. The reason could be the lack of specific and widely held standards for characterizing these materials. During the last decade, just a few recommendations and guidelines (American [62] and European [55]) were published for FRCMs, with testing configurations not necessarily equivalent. As mentioned previously, the experimental setup, mainly the specimen grip method (clamping or clevis), influences the results, with the clevis method roughly underestimating the tensile strength. Indeed, investigations still primarily rely on laboratory trials and empirical approaches, specifically in the case of natural FRCMs.
- The UTS and MOR of composites reinforced with p-aramid textiles were twice higher than the other counterparts, making those suitable for structural-oriented applications, mainly retrofitting existing masonry elements (few guidelines were published for this

purpose [63,64]). Nonetheless, the economic/environmental impacts of these synthetic reinforcements (mainly p-aramid or carbon) pose a challenge and a potential barrier.

- AR-glass FRCMs emerged as a suitable substitution for energy-intensive and high-cost p-aramid or carbon FRCMs [51], reaching UTS and MOR in the range of 8–18 and 15–20 MPa, respectively. However, the toughness and strain capacity of these composites were limited.
- Vegetal textiles could be employed to boost sustainability, toughness (energy absorption), and ductility. Although reaching a lower range of UTS (5–12 MPa) than glass FRCMs, the MOR and especially the flexural toughness were superior, making these a proper candidate for stand-alone building components with low-intermediate structural responsibility (e.g., building envelopes and precast panels) or retrofitting of the built heritage with weak substrate [65].

Considering durability (especially in the case of glass and natural-based textiles) and sustainability performances, it is seen justifiable to develop more eco-friendly FRCMs by resorting to low carbon matrices (maximum 50% PC) and affordable/easy-fabrication textiles. Nonetheless, each FRCM product with a different/innovative mortar or fabric type must undergo the qualification procedure (especially for structural purposes) before its transfer to the construction market.

3. Materials fabrication and testing methods

3.1. Characterization of laminated FRCM composites

Light and thin nonwoven fabrics were produced from 100% shredded fibers from textile waste (TW) of fire-proofing T-shirts worn by firefighters. This TW fiber, with a length of less than 7 mm, consisted mainly of aramid fibers (93% meta-aramid and 5% p-aramid) with 2% antistatic fibers. As shown in Fig. 2a, these meta-aramid recycled fibers were dyed (this is why they had a bluish color instead of the typical yellowish color of aramids), which may boost the hydrophobicity behavior. The aramid textile waste (ATW) nonwoven fabric (with a thickness of ~1.5 mm and an areal weight of 145–155 g/m^2) was produced by carding and needle punching techniques by using the DILO OUG-II-6 double needle machine as described elsewhere (Fig. 2c) [66]. The tensile rupture load of the needle-punched nonwoven ATW fabric was reported to be around 36 N.

The laminated compression-mold composite plates of 300 mm × 300 mm × ~ 10 mm were fabricated by stacking the fabric layers while simultaneously employing dewatering treatment (adapted from the Hatschek process), as explained in more detail in the previous work [36]. Briefly, suction was applied to the perforated mold while layers of fabric previously impregnated in the fluid matrix (Fig. 2e) were inserted cross-oriented between the thin outer layers of PC paste, CEM I-52.5 R (provided by Cementos Molins, SA) mixed with water in an initial ratio of 1.0. After being compressed under the constant pressure of 30 bar (to reduce extra water and the

Fig. 2. Fabric and composite production: a) Shredded ATW; b) Shredded fashion TW; c) nonwoven ATW fabric; d) nonwoven HTW fabric; e) Impregnation of the fabric in the matrix; f) Final laminated plates.

Table 3
Mix proportions and nomenclature of the samples.

Sample	ATW4	ATW6	HTW6
Cement [gr]	1100	1300	1300
Water [gr]	1100	1300	1300
$(w/b)_{final}$	0.55	0.55	0.45
Plate Thickness [mm]	10	12	10

porosity), the unmolded plates (Fig. 2f) were cured in 20 ± 1 ° C water for 28 days.

The durability of FRCMs (especially those including natural-based fibers) is still a significant concern; thus, reliable methods must be further developed to assess long-term behavior. While most available studies on the durability of FRCMs focused on accelerated aging through hot-water immersion, cyclic aging (dry-wet or freeze-thaw) could be more realistic to simulate changing climatic conditions (e.g., rain, heat, freeze, temperature changes) [67]. Thus, according to EN 12467 [68], developed composite plates underwent 25 cycles of FT and 25 cycles of DW accelerated aging in the CCI climatic chamber to simulate their long-term performance. Each FT cycle lasts 6 hours and consists of a temperature shift from 20 to −20 ° C, while each DW cycle entails 6 hours of drying at 60 ° C with 20% relative humidity followed by 18 hours of immersion in 20 ° C water.

Unaged and aged plates were machined into six specimens (300 mm × ~50 mm × ~10 mm) to determine the tensile and flexural load-bearing capacities. A four-point bending (4PB) test was applied with an Incotecnic universal testing machine with a span length of 270 mm, according to RILEM TFR 1 [69] and TFR 4 [70], while the direct tensile test (gauge length of ~200 mm) with a Metrotec universal testing machine (followed the methodology of RILEM TC 232-TDT [55]. Mechanical clamping of grips was applied at the clamping wedges of the composite while rubber tabs with ~2 mm thickness and the same width as the specimens were placed at the end of coupons to avoid localization of stresses at the load transition region. As mentioned in [57], if the lateral pressure induced by clamping grips is appropriate, the slippage of the textile is prevented, and the imposed bending is negligible. For each test configuration, the following parameters were estimated as described in depth in [34]: the breaking stress of the matrix (first crack strength from the stress-strain curve) known as the limit of proportionality (LOP) in flexion or bend-over point (BOP) in tension, the maximum stress of the composite known as modulus of rupture (MOR) in flexion or ultimate tensile stress (UTS) in tension, the flexural or tensile stiffness as the slope of the force-displacement or stress-strain curves in the pre-cracked zone (E_F or E_T), and the toughness index (I_{GF} or I_{GT}) as the specific fracture energy through the area under the force-displacement curve divided by the cross-section. The strain in the tensile test was measured based on the global displacement of the crosshead.

The mix design and sample nomenclature are displayed in Table 3. ATW4 and ATW6 were those composites reinforced with 4 and 6 layers of TW fabrics from fire-protecting clothes (mainly meta-aramid fibers). Moreover, HTW6 referred to the FRCM plate reinforced with six layers of hybrid fabric (65% fashion TW clothes + 35% long flax) based on the previous study (Fig. 2b,d). The recycled short fashion TW fibers (majority less than 4 mm) comprised 70% cotton and 30% polyester; thus, the HTW fabric comprised 80% vegetal fibers (45% cotton + 35% flax) and 20% polyester. The forced-aged plates had the suffixes DW and FT.

3.2. Characterization of recycled aramid TW short fibers

Substituting the partial PC with pozzolans/SCMs could not only improve the cementitious composite's durability (specifically those reinforced with natural-based fibers) by decreasing the matrix's alkalinity (calcium hydroxide or portlandite) but also lead to the production of low carbon cement-based materials as a short-term solution [15,65]. Since the mechanical properties of the fabricated composites with 100% PC degraded after DW aging (see Sections 5.1 and 5.2), the behavior of shredded ATW fibers immersed in the PC matrix and the blended one with 0–50% SF (provided by Arcillas Refractarias, S.A ARCIRESA, which has more than 93% silica) was studied.

To this end, accelerated DW aging (5 and 10 cycles) was applied to the short fibers impregnated with the blended paste (100% PC, 90% PC, 70% PC and 50% PC), and the tensile properties of the fiber were assessed. Initially, the fluid pastes (water-to-binder ratio of

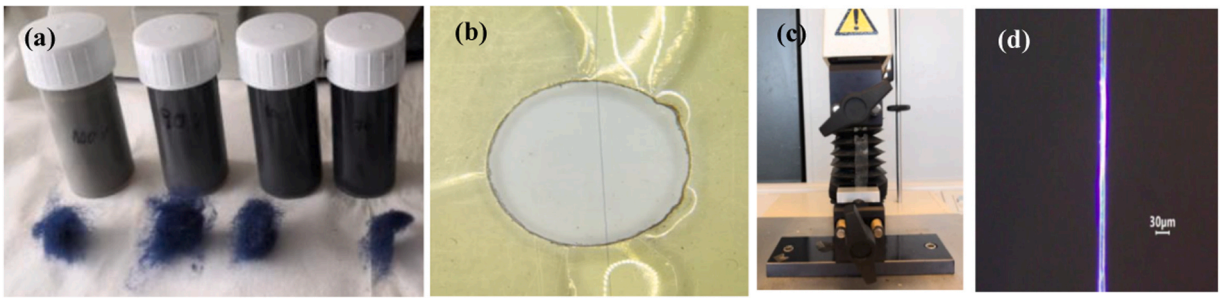

Fig. 3. a) Test tubes with different pastes; b) Individual fiber observed with a magnifying glass; c) Preparation of the individual fiber at the testing machine; (d) TWA fiber under the optical microscope at x100 magnification.

2.0) were continuously stirred at a constant speed for seven days to remain in a liquid state all the time (not harden quickly), even after aging. Subsequently, the prepared pastes were poured into small tubes (Fig. 3a), and a handful of short fibers were inserted inside prior to starting the accelerated aging process. Each DW cycle, lasting seven days, consisted of drying the uncovered tubes (with the fibers inside) in the oven at 60 ºC for four days, followed by saturating in 20 ºC water for three days. At the end of the 5 and 10 cycles, ten individual fibers from each test tube were collected for the tensile characterization test. The tensile test was carried out using the texturometer TA.XTPLUS/30 (Stable Micro Systems), using A/TG-R accessory tensile grip, with a load cell of 5 kg and a 2 mm/min test speed according to ASTM C1557–20 [71] (Fig. 3b-d). Using a magnifying glass, the ends of the fibers were adhered with cyanoacrylate glue to a plastic strip (mounting tab), while the central part of the fiber was free and straight. Once the samples were placed in the tensile grip, the plastic's edges were cut so that the fibers were released at both ends, thereby the tensile force applied to them directly. Further, the intact shredded TW fibers were tested without immersion in the paste.

The following parameters were assessed based on the tensile test: the tensile strength of the fiber (T_s) by dividing the maximum tensile force by the cross-section area (measured by analyzing the image), the modulus of elasticity (E_s) from the elastic region where the elongation of the fiber is proportionated to the tensile force, and the specific energy, i.e., the amount of energy absorbed by the fiber during the test (corresponds to the area under the force-displacement curve divided by fiber area). It should be mentioned that the diameter of the ATW fiber, and consequently the area, was measured by placing it in the optical microscope using ToupView software (image analysis system combined with a reflected light microscope [66]).

4. Results and discussion

4.1. Flexural properties of laminated composites

The representative flexural curves of unaged samples (ATW4 and ATW6) are shown in Fig. 4a and compared with HTW6. As can be observed, all composite plates exhibited deflection-hardening behavior with noticeable deformation through the formation of multiple cracks following the linear elastic regime. As a result, the composites could withstand additional stresses beyond the LOP (strength of the uncracked zone) due to the interaction between the matrix and nonwoven textiles (during the crack development stage). The specimens eventually failed after completing the cracking pattern due to fiber pull-out at the fracture section (in the cracked stage). Regarding composites after exposure to DW aging (Fig. 4b), the flexural curves of all samples demonstrated rather a brittle tendency, i.e., the deflection capacity of ATW6 and HTW6 were limited to 5 and 25 mm, in comparison to 12 and 35 mm in unaged condition, respectively. As for accelerated FT cycles (Fig. 4b), the bending curves were virtually similar to those of unaged ones, showing high deflection capacity with failure that happened by the gradual failure of the reinforcing fibers (deflection softening). Thus, the adverse effect of DW cycle aging on ductility/toughness was more evident compared to FT aging.

Fig. 5 gathers all the mechanical parameters from the 4PB test for the studied panels. The HTW6 composite plate proved higher values in almost all characteristics than the counterparts with ATW fabrics, although both types of reinforcement enhanced the composites' post-cracking behavior (i.e., MOR/LOP$\geq$1.9). As for unaged composites with six layers of reinforcements, the post-cracking parameters of HTW6, i.e., MOR and I_{GF}, were significantly higher than ATW6 (37% and 127%, respectively). Indeed, these higher post-cracking parameters were mainly related to higher reinforcement contribution (MOR/LOP ~1.9 for ATW6 and ~2.6 for HTW6) since the pre-cracking properties of both composites (LOP and E_F) were in the same range. This performance proved that hybrid fabric (made up of cotton + polyester + flax) was more compatible with the cement matrix, and the penetration of the matrix into HTW was better, leading to more homogeneous composites with efficient matrix-fiber adhesion. As reported by Tran. et al. [39], hydrophilic fibers form a stronger bond with the matrix in comparison to those hydrophobic. However, it should be noted that since the

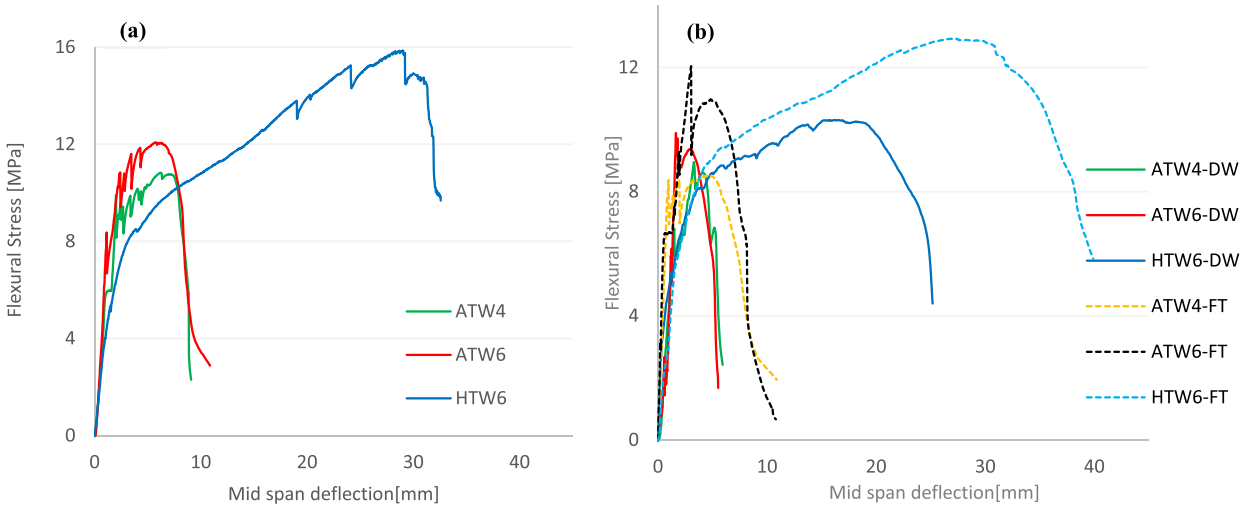

Fig. 4. Representative flexural stress–deflection curves of all composites: (a) unaged; (b) aged.

recycled fibers were recovered from finished cloth, there could be differences in the fiber surface hydrophobicity. Indeed, the wettability of the fabrics containing cotton and/or flax was higher than those containing mainly aramid, especially the recycled meta-aramid fibers in this study, which were dyed and coated, that led to lower wettability. Further, flax fibers (60 mm) in HTW were longer than recycled TW fibers and, consequently, the former generated greater adhesion with the matrix due to greater surface area [39]. Regarding the number of reinforcement layers, six layers of ATW reinforcement had higher post-cracking properties than four layers (12% and 44% for MOR and I_{GF}); a similar trend by increasing the textile layers was reported in other studies [36,50].

As can be concluded from Fig. 5, post-cracking values of the composites were evidently reduced after DW aging. i.e., ATW4, ATW6, and HTW6 lost MOR by 25%, 16%, and 37% (respectively), whereas those samples' toughness dropped by 47%, 51%, and 39%. This loss in post-cracking parameters indicated that these reinforcements are susceptible to extreme weather conditions due to fiber degradation and embrittlement. Indeed, $Ca(OH)_2$ ions from the PC matrix slowly attack the fibers in an unaged state, while repeated exposure to DW cycles causes the cement matrix's capillary pores to alternately fill and empty with alkaline pore water, speeding up the attack of the hydration product (mostly portlandite) to the fibers and causing fiber brittleness [72]. Comparing HTW6 and ATW6 in DW conditions, the post-cracking parameters of the former decreased more (on average 5%), probably due to a higher amount of natural fibers in HTW [73]; however, HTW6-DW still had higher post-crackling values, especially toughness (around three times). Regarding the pre-cracking characteristics of the first stage (uncracked zone), LOP and E_F in all composites varied by less than 15% since the matrix mainly governed those parameters while the DW cycles affected mainly fibers.

As for FT aging, the MOR dropped by 5%, 1%, and 20% for ATW4, ATW6, and HTW6 (respectively), while the energy absorption fell by 16%, 4%, and 23% for those composites. Thus, FT cycles were less devastating for cement composites since the incorporation of the fibers enhanced the material's porosity while giving greater flexibility [38], resulting in the progressive release of the tension of water's expansion during the freezing phase. Regarding pre-cracking parameters, similar to DW aging, these values increased by 15%, possibly because of the continual hydration reactions throughout aging.

Table 4 summarizes the flexural properties of various unaged nonwoven FRCMs (only optimum layers of each composite were gathered) in inorganic matrices based on previous studies. As reported, the tensile rupture load of nonwoven fabrics (including flax, HTW, and ATW) varied in the range of 4–36 N. On average, the cement-based composites reinforced with flax or HTW (flax + fashion TW) fabrics had higher post-cracking parameters (MOR of ~16 MPa and toughness of ~10 kJ/m^2) than the ATW counterparts. As already explained, flax and fashion TW fibers were more hydrophilic than aramid ones, leading to better bonding and matrix penetration. Further, the existence of long flax fibers positively affected the interface and the behavior of the composite. Hornificated flax fibers proved the best performance (MOR of ~20 MPa and toughness of ~12 kJ/m^2) since those reinforcements had the highest affinity to water due to the removal of hydrophobic compounds from the surface during this physical treatment [74]. In comparison to the flexural performance of woven FRCMs (Table 2), the post-cracking parameters of nonwoven fabric composites (100% flax or HTW) are comparable to those reinforced with woven fabrics, including 100% PP, 100% AR glass, or vegetal, apart from those including p-aramid textiles. Specifically, the toughness (energy absorption) of nonwoven composites is superior to that of the reported AR glass composite (with a toughness of 2–4 kJ/m^2). Indeed, the correlation between textile strength/modulus and cement composite properties (i.e., post-cracking parameters) is not necessarily straightforward. The properties of the composite are mainly influenced by the geometry and form of the fabric, as well as the bond that develops between the fabric and the cement matrix, and less by fabric strength/modulus [75]. Thus, considering the sustainability aspects (economic and environmental), nonwoven fabrics could be promising options compared to expensive AR-glass or polymeric textiles.

Table 5 summarizes the data on the residual flexural properties of accelerated-aged FRCMs, mainly natural-based composites, under cyclic conditions. The durability of vegetal FRCMs in both PC and blended matrix under 25–100 DW cycles and hot-water immersion was investigated by Toledo Filho et al. [53] and Silva et al. [77]. As observed in the PC matrix composites, there was no meaningful difference in post-cracking parameters loss between 25 and 100 DW cycles; MOR and I_{GF} decreased by around 60% and 98%, respectively. Indeed, after 10 DW cycles, the mineralization and embrittlement of the cellulosic fibers happened, while the main mechanical losses occurred during the first 5 DW cycles, as reported by Mohr et al. [78]. Moreover, the toughness (energy absorption) was the main parameter adversely influenced by DW aging, reduced by up to 100%, as already concluded in the present study. On the other hand, the low calcium hydroxide (CH) matrix treated with 50% SCMs could perform better than the PC matrix after DW aging; MOR increased by 30% and toughness reduced by only 25%. Microstructure analysis done in [53,77] confirmed that in the PC composite, the fiber-cells were mineralized, possibly due to the high Ca^{2+} concentration, while the CH-free composite showed no signs of fiber deterioration due to much lower Ca^{2+} concentration inside the fiber-cells. Further, Toledo Filho et al. [72] highlighted that the uni-directional long sisal fibers (FRCM) were less adversely affected than short fibers (ECC) due to the lower number of endpoints and smaller surface area, which caused the slower penetration of CH to the fibers.

Regarding the durability of synthetic FRCMs, Yin et al. [79] studied the long-term behavior of ternary matrix reinforced with coated two-directional knitted carbon/glass yarns after exposure to various chloride DW and FT cycles. They concluded that the rise in chloride DW and FT cycles decreased interfacial bonding strength between the textile and fine mortar, gradually decreasing the pre- and post-cracking load capacity (LOP and MOR). As for the aged nonwoven FRCMs, flax composites containing calcium aluminate cement matrix treated with 10% MK could maintain the post-cracking performance after 250 DW cycles [59]. Hornificated flax and HTW fabrics in the PC matrix lost about 40% of the toughness after 25 DW cycles, while this value was 80% and 50% for the untreated falx and ATW composites, respectively [36]. The HTW composite treated with 30% SF could improve the post-cracking performance by 30% compared to the PC matrix [34]. Furthermore, the loss induced by FT cycles in post-cracking parameters was less than DW simulations in all composites (see the percentage change in MOR and I_{GF} in Table 5).

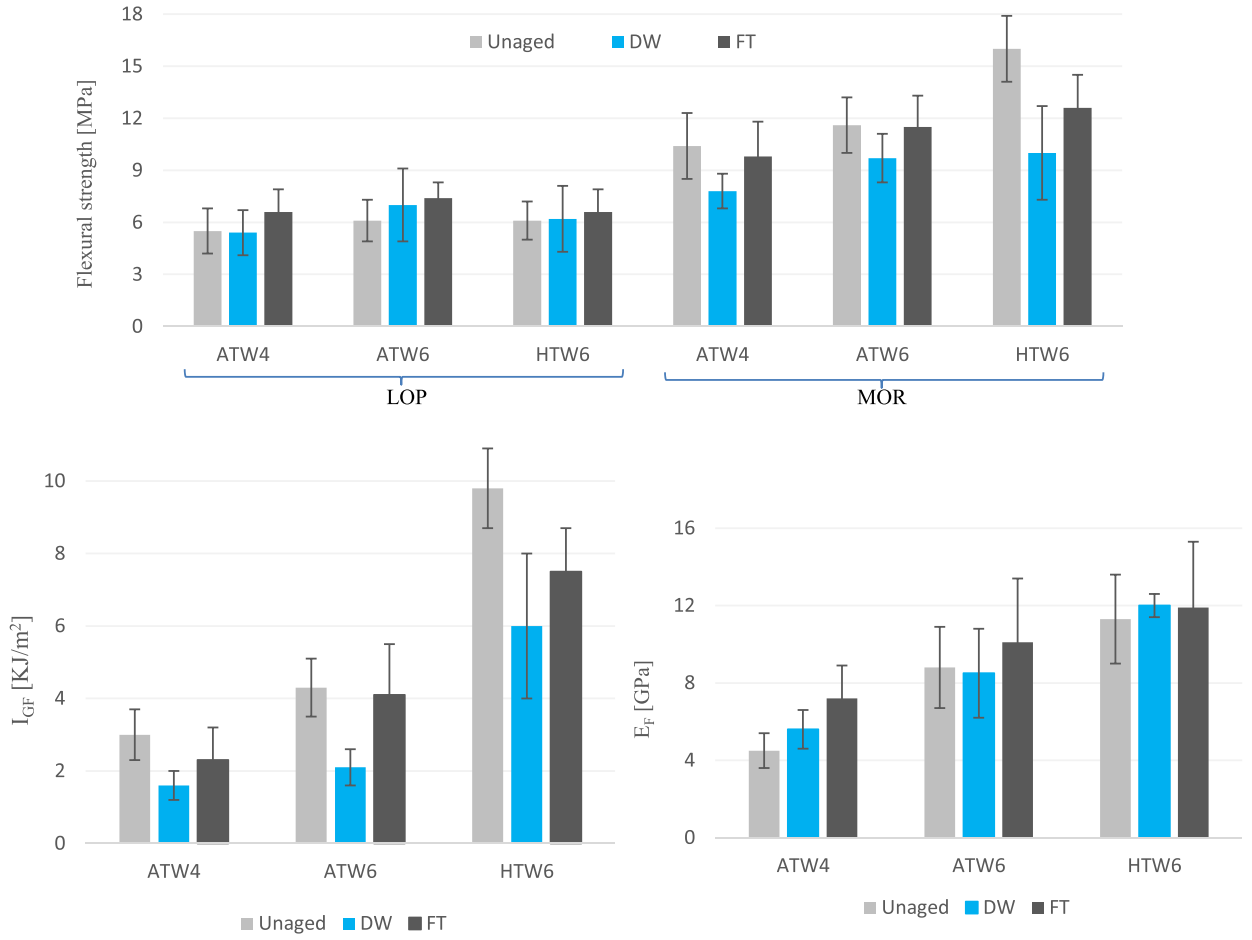

Fig. 5. Flexural properties of composite panels from 4-point bending test.

4.2. Tensile properties of laminated composites

Fig. 6 illustrates the tensile representative curves of the nonwoven composite panels. As can be seen, panels in unaged condition (specifically those incorporating six layers) presented ductile behavior by forming multiple cracks after the linear elastic regime. Thus, after reaching BOP in the elastic zone (resistance of uncracked stage in which the matrix mainly contributes to load-bearing capacity and stiffness), the composites could tolerate further loads due to the interaction between the matrix and the nonwoven fabrics in the crack development stage (in which both matrix and textile govern the performance). Ultimately, following the development of the crack pattern, the specimens experienced failure in the cracked stage (in which the fabric mainly dominates the performance) due to fiber pull-out at the fracture section in the middle area of the specimen (Fig. 1f). It should be noted that the fiber pull-out mechanism in the developed nonwoven FRCMs was not telescopic since this occurred due to the weak core-to-sleeve interaction within the multi-filament textile yarns. Indeed, the structure of nonwoven fabrics differs from that of woven multifilament yarns/threads as it is produced by entangling the discrete fibers.

As to DW-aged samples (Fig. 6b), the tensile curves of all composites showed less ductile behavior, i.e., lower strain capacity (failure strain capacity for ATW6 and HTW6 reduced by 43% and 57%, respectively). Indeed, bilinear performance was predominant in comparison to the ideal trilinear stress-strain behavior (limited cracking zone hardly visible), this probably being due to the reinforcement degradation. Other reasons for the lack of cracking formation stage, as reported in [57], could be related to the high-resistant mortar matrix, which discourages a uniform distribution of stress along the FRCM system, or the low reinforcement ratio of the composite. Further, if the composite only experienced one major crack, the second and third stages are hardly identifiable in the stress-strain relationships [45]. Thus, while the experimental expected response is trilinear, distinct/complex behavior may be observed due to heterogeneity/various constituent materials [80]. For this reason, the stress-strain relationship of FRCMs could also be assumed as bilinear, based on the AC434 recommendation [62]. As for forced FT cycles (Fig. 6b), the curves were relatively similar to the unaged ones, showing a more noticeable multiple cracking zone, i.e., after the cracking stress of the matrix, the load increased by forming several cracks; thereby, the ultimate failure load is higher than the one associated with the matrix cracking onset.

The mechanical parameters obtained from the direct tensile test of various nonwoven FRCMs, including unaged/aged ATW (4 and 6

layers in PC), unaged/aged HTW (6 layers in PC and blended PC-30%SF), and unaged hornificated flax (5 layers in blended PC-10%SF) are compared in Fig. 7. Like flexural behavior in unaged conditions, the HTW6 proved a higher value than ATW6 (roughly two times in all parameters). However, both types of fabrics effectively enhanced the composites' post-cracking behavior (UTS/BOP $\geq$1.9). On average, the cement-based composites reinforced with 5–6 layer hornificated flax or HTW fabrics had higher post-cracking parameters (with UTS of ~7 MPa and toughness of $\geq$40 kJ/m^2) than the ATW6 counterparts (with UTS of ~3.7 MPa and toughness of ~25 kJ/m^2). As explained in the previous section, the higher post-cracking parameters of the HTW and flax composites were related to better fabric-matrix compatibility, penetration and bonding. Further, the high-length flax fibers avoided composite strength drop by more effective microcracks' arresting [81]. Besides, it should be mentioned that the average value of the cracking strength of the ATW composites was inferior to those observed for HTW or flax panels, which may be associated with the higher porosity and/or larger pore structure of ATW panels. As Tran et al. explained [14,15], fibers with lower wettability (greater hydrophobicity) may cause the formation of larger pores compared to hydrophilic fibers (vegetable ones) since the moisture-retaining capacity of the latter may act as a local reservoir, i.e., supplying moisture to the surrounding matrix for further hydration over time, this leading to denser microstructure with finer pores.

Regarding the number of reinforcement layers, similar to flexural performance, the ATW6 composite showed higher post-cracking parameters than ATW4 (20% and 100% for unaged I_{GT} and UTS, respectively). Indeed, by increasing the number of reinforcing layers, the energy accumulates faster during the multiple-cracking phase, leading to more cracks and toughness [82]. The formation of new cracks depended on the ability to transfer stresses throughout the material; thus, more reinforcing layers indicated higher stress transfer channels. Similarly, Paul and Gettu [81] noted that glass FRCM with only a single-layer textile demonstrated strain-softening behavior while increasing the reinforcement layers to 4–5 enhanced the distributed cracking phase with strain-hardening performance. Contrary to the present study, those authors concluded that a higher reinforcement ratio led to lower ultimate strain capacity due to the high stiffness of glass textiles. Likewise, Larrinaga et al. [80] reported that by increasing the quantity of textile layers, the number of cracks increased while the crack distance diminished.

After DW aging, UTS of ATW4, ATW6, and HTW6 were reduced by 32%, 29%, and 48%, respectively, while the toughness of those samples decreased by 59%, 74%, and 85%. This loss demonstrated that this type of reinforcement, especially HTW, was vulnerable to severe weather conditions as a result of the deterioration and brittleness of the fibers. As explained in the previous section, the movement of OH^- and Ca^{2+} ions from the cement portlandite to the fibers occurs slowly under a stable environment. Nevertheless, subjecting the material to multiple cycles of DW prompts the capillary pores within the cement matrix to alternately fill and empty with alkaline pore water, which speeds up the transfer of the hydration product to the fibers, leading to fiber embrittlement. As the HTW fabric had a high amount of vegetal fibers (80%), it was more vulnerable concerning ATW, considering cellulose-based fibers deteriorate more significantly than synthetic ones. All plates' pre-cracking properties (BOP and E_T) varied less than 10% since those parameters were mainly affected by the matrix properties (considering the low stiffness and volume fraction of fibers).

Regarding forced FT cycles, the detrimental impact of this type of aging was comparatively lower than that of DW cycles., especially for ATW plates.; the UTS decreased by 6%, 3%, and 30% for ATW4, ATW6, and HTW6 (respectively), while the energy absorption reduced by 15%, 39%, and 60% for those plates. Indeed, during FT cycles, the alkalinity of the matrix caused a lower degree of fiber degradation when compared to aging resulting from DW, as observed from microstructural analysis in previous research [34]. Finally, the values of pre-cracking parameters exhibited a slight increase, which may be attributed to the late hydration of unhydrated cement particles through aging. Fig. 8 summarizes the deviations in tensile parameters of 6-layer nonwoven FRCMs (ATW and HTW) after cyclic aging to better compare the unaged and aged conditions, obviously observing that the FT cycles had less adverse effect than DW cycles. Further, as reported, aged HTW composites treated with 30% SF showed higher post-cracking parameters (45% on average) than those aged in the PC matrix [34]. It should be mentioned that no other comprehensive studies, to the authors' knowledge, were found on the tensile performance of cyclic-aged natural-based woven or nonwoven FRCMs. However, few studies have been conducted on the cyclic-aged tensile performance of synthetic FRCM, especially with glass textiles. Among those, De Munck et al. [67] reported that the UTS of AR glass FRCM after 30 FT cycles reduced by only 4%, while this reduction was 32% and 9% for 80 heat-rain and 5 heat-cold cycles, respectively, confirming that the FT aging was less aggressive even for synthetic FRCMs.

Compared to the tensile performance of woven synthetic/vegetal FRCMs (Table 1), the elasticity modulus and UTS of synthetic FRCMs (especially those included p-aramid) were significantly higher than nonwoven composites, two orders of magnitude and four times, respectively. The UTS of 100% PP, 100% AR glass, or vegetal woven FRCMs could be comparable to nonwoven ones (flax or HTW), though the values of formers were around two times higher. The only superior parameter in nonwoven FRCMs was the ultimate strain capacity or ductility, especially compared to AR glass composite. The natural woven and nonwoven FRCMs failed from crack widening and fiber pull-out, leading to higher flexibility and ductility than glass composites (see Failure modes in Table 1).

Regarding the two typical configuration tests (4PB and uniaxial tensile) applied on FRCMs, it should be noted that all calculated parameters, except the toughness index, had noticeably higher values for the 4PB test, i.e., the first crack strength, the maximum strength and the elastic stiffness had averagely higher quantities by 3.2, 3.1, and 74.7 times, respectively. Only the toughness index had a considerably higher amount in the direct tensile configuration, up to 4 times. A similar trend was observed in other studies [32,34,49], while specifically in [49] the authors highlighted that the saturation crack spacing under flexural loads was twice with respect to those under tensile loads. Indeed, the whole cross-section is under tension in direct tensile configuration, while in flexural mode, part of the cross-section is under compression, where the matrix performs better. Further, in flexure, the main dominant parameters influencing the behavior are delamination, interfacial bond and matrix penetrability, while in tension, textile properties also have a pivotal role [44,75].

Table 4
Data Summary of the unaged flexural properties of 5–6 layer nonwoven FRCMs.

Nonwoven fabric type (V_f or W_f if reported)	Tensile fabric rupture load [N]	Matrix type	Flexural test set-up of composites			Composite properties					REF
			3PB/ 4PB	Specimen dimensions [mm]	Span length [mm]	MOR [MPa]	LOP [MPa]	I_{GF} [kJ/ m^2]	$E_{1\,F}$ [GPa]	ε_F [%]	
Hornificated flax - 6 layers (W_f = 9%)	16	PC- CEM I	4PB	300× 50 × 10	270	19.8	7.6	12	11.4	8.6	[36]
Flax - 6 layers (W_f = 13%)	10					15.7	4.4	9.2	7.3	7.0	
HTW - 6 layers (W_f = 5.5%)	4					16.0	6.1	9.8	11.3	6.7	
	4	PC- CEM I + 30% SF				14.4	5.3	8.6	10.7	6.9	[34]
Flax - 5 layers	N.A.	Calcium aluminate cement + 10% MK		300× 50 × 12		16.3	8.1	11.1	10.7	8.1	[59]
ATW - 6 layers (W_f = 11%)	36	PC- CEM I				11.6	6.1	4.3	8.8	2.5	Present Study
Hornificated flax - 6 layers	16	Slaked lime + 20% MK	3PB	150× 50 × 10	120	4.85	3.3	3.2	0.4	9.2	[76]

Table 5
Data Summary of the accelerated cycling aging effect on the flexural properties of the FRCMs.

Textile type	Matrix type	Type of accelerated aging test	Percentage change in 4PB parameters for aged FRCM concerning unaged			REF
			MOR	LOP	I_{GF}	
Uni-directional long-aligned sisal - 5 layers (V_f=10%)	100% PC	25 DW cycles	-69.9	+8.8	-98.4	[53,77]
		50 DW cycles	-71.7	+2.4	-99.5	
		75 DW cycles	-61.1	+40.7	-98.1	
		100 DW cycles	-60.1	+44.4	-98.6	
	50% PC + 30% MK + 20% calcined waste clay brick	25 DW cycles	+10.5	+26.4	-11.2	
		50 DW cycles	+8.0	+9.3	-17.7	
		75 DW cycles	+18.3	+52.4	-25.8	
		100 DW cycles	+29.0	+65.0	-15.7	
Coated bi-directional knitted hybrid carbon/glass	70% PC + 25% FA + 5% SF	90 chloride DW cycles	-7.3	-16.2	N.A.	[79]
		150 chloride DW cycles	-9.4	-44.1	N.A.	
		50 chloride FT cycles	-0.9	-1.9	N.A.	
		90 chloride FT cycles	-28.8	-13.8	N.A.	
Flax nonwoven - 5 layers	Calcium aluminate cement + 10% MK	250 DW cycles	-4	-24	-12	[59]
Hornificated flax nonwoven- 6 layers (W_f = 9%)	100% PC	25 DW cycles	-45	-8	-40	[36]
Flax nonwoven - 6 layers (W_f = 13%)			-50	+18	-82	
HTW nonwoven - 6 layers (W_f = 5.5%)	100% PC	25 DW cycles	-37	+2	-39	[34]
		25 FT cycles	-20	+3	-23	
	PC- CEM I + 30% SF	25 DW cycles	-1.5	+10	-6	
		25 FT cycles	+6	+11	+1	
ATW nonwoven - 6 layers	100% PC	25 DW cycles	-16	+14	-51	Present Study
		25 FT cycles	-1	+20	-4	

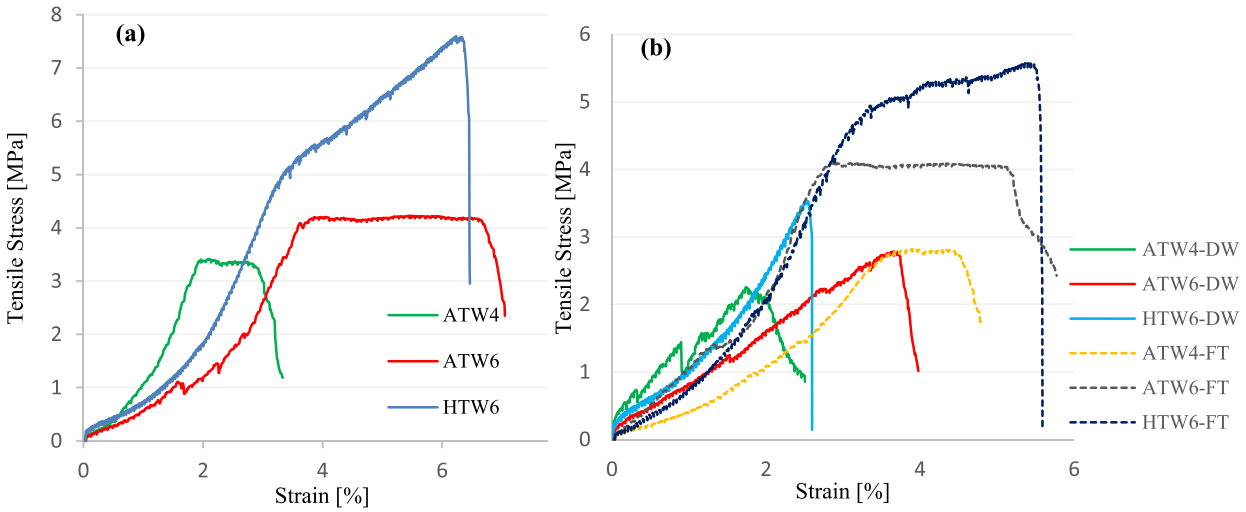

Fig. 6. Representative tensile stress–strain curves of all composites: (a) unaged; (b) aged.

4.3. Tensile characterization of short aramid TW fibers

The tensile properties of the recycled aramid TW fiber, both intact (unimmersed) and aged ones (after 5 and 10 DW cycles), are gathered in Table 6. Notably, the diameter and area of the single ATW fiber were measured as 15 μm and 176.7 μm^2, respectively. The intact meta-aramid fiber recovered from TW showed a tensile strength (T_s) of 268.9 MPa and a modulus of elasticity (E_s) of 5.2 GPa. However, based on the literature, T_s and E_s of p-aramid fibers were~3000 MPa and 70–110 Gpa, respectively, with a density of around 1.4 g/cm^3 [12,83]. Therefore, the recycled meta-aramid fiber in the present study had ten times lower mechanical properties than the industrial synthetic counterparts. This recycled fiber could be comparable with vegetal fibers (such as flax, hemp, jute, and sisal) with T_s in the range of 200–650 MPa and E_s of 5–50 GPa [29,84,85]. The recycled Nomex and Kevlar fibers from TW in this study of [14] had T_s as 410 and 1460 MPa with E_s of 0.9 and 55 GPa, respectively.

As observed in Table 6, the fibers' resistance was reduced after aging, especially for those immersed in 100% PC (by 18 and 24% after 5 and 10 DW cycles, respectively). Nonetheless, the fibers impregnated with 30–50% SF blended matrices could roughly maintain their resistance, i.e., the loss was only by 8% after being subjected to 5 DW cycles and 18% after 10 cycles (see Fig. 9). Indeed, treating the PC with a high amount of SF reduced the matrix's alkali content; therefore, a lesser adverse effect was observed on the fibers' resistance. As for energy absorption variation, the trend was compatible with tensile strength. In other words, immersed fibers in SF-treated matrices had almost equal (or even higher) toughness as the intact fiber after five DW cycles (the range varied from 67.9 to 75.7 J/m^2), while the one impregnated with 100% PC had 15% loss respect to intact one. However, the specific energy loss after ten DW cycles was roughly significant even for SF-treated matrices (25–38%), with the highest loss for the 100%PC sample (42%). Contrary to the previous parameters, the modulus of elasticity of the fibers degraded more significantly after five cycles (27–34%) with respect to 10 cycles (19–25%). Further, no evident trend was observed in the fiber stiffness by increasing the amount of SF. Similarly, Correia et al. [86] concluded that no linear correlation existed between the elastic modulus of vegetal fibers and the increase in aging cycles. Finally, it should be noted that the tensile parameters of fibers presented a relatively high scatter; this can be reasonably attributed to the intrinsically irregular morphology (heterogeneity) as well as deriving from recycled substances. A similar noticeable dispersion of properties was observed for untreated vegetal fibers [29].

5. Conclusions

To reach sustainable development goals, the circular economy approach based on recycling and reusing is gradually substituting the linear economy. In this context, meta-aramid fibers recovered from protective clothing (ATW) were used in this research as reinforcement of cement-based matrices, and the tensile and flexural resistance of the resultant fabric-reinforced cementitious matrix (FRCM) were characterized after these were exposed to various environmental conditions (unaged, dry-wet and freeze-thaw aged). The experimental results were compared with other results obtained from experimental programs on FRCMs reinforced with synthetic (aramid, PP, and glass textiles) or vegetal fabrics. The primary outcomes derived from this experimental program and the comparative analysis are as follows:

- The recycled short shredded ATW fiber (mainly composed of meta-aramid) presented tensile strength and modulus of 268.9 MPa and 5.2 GPa, respectively, these being comparable to natural-based fibers. These values were significantly less (one order of magnitude) than synthetic p-aramid fibers.

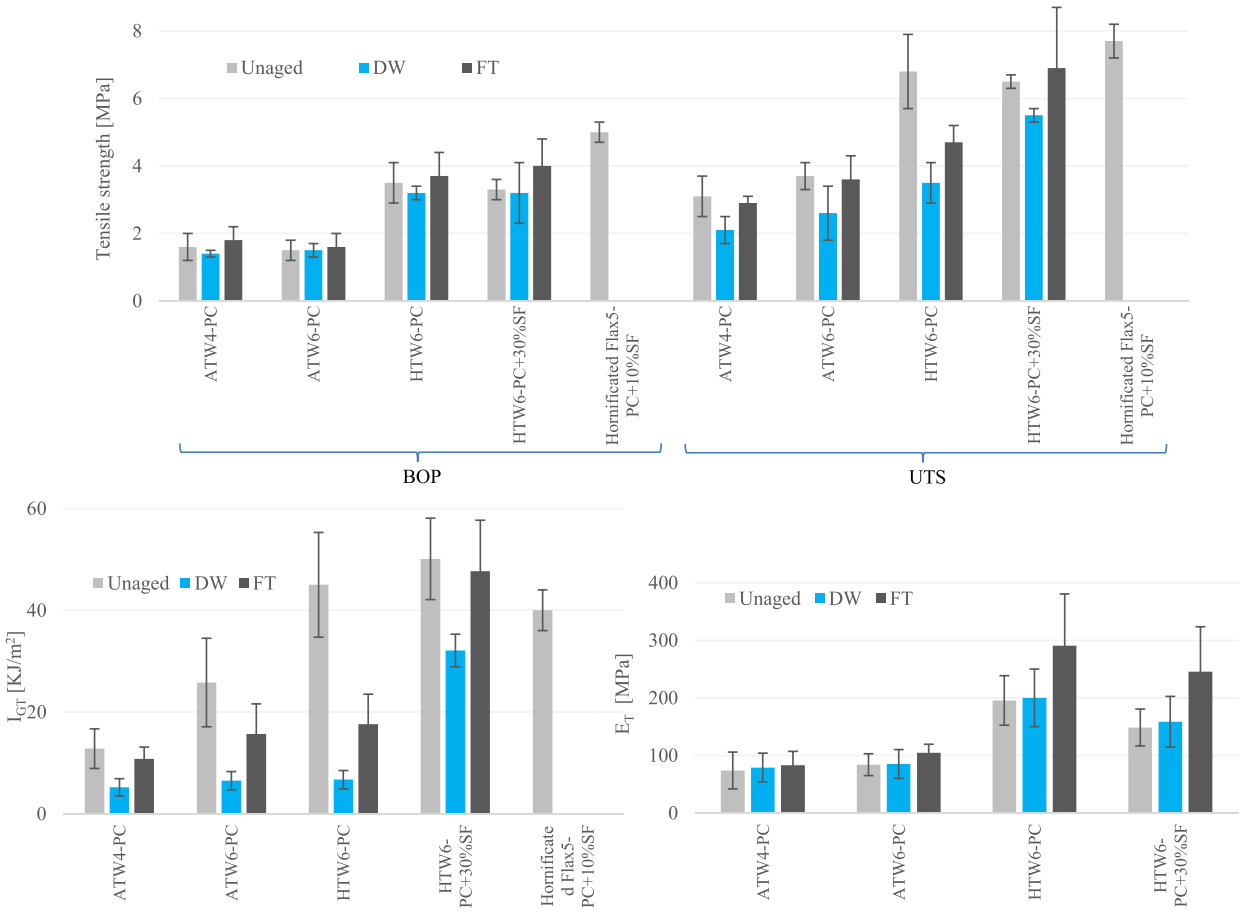

Fig. 7. Tensile properties of nonwoven FRCMs (The data of "HTW6- PC+30%SF" and "Hornificated Flax5- PC+10%SF" samples were adapted from [34] and [32], respectively, while the latter sample had limited data only in unaged condition).

- The tensile properties of recycled aramid fibers degraded by forced dry-wet (DW) simulation in the Portland Cement (PC) matrix, on average, 20% and 30% after 5 and 10 cycles, respectively. However, treating the matrix with 30–50% silica fume (SF) could improve the aged performance by 10%.
- The composite panels containing ATW nonwoven fabrics showed lower post-cracking mechanical values than other nonwoven FRCMs made from 100% flax or hybrid fashion TW (HTW), on average (in flexural and tensile) by 40% in ultimate strength and 50% in toughness. Vegetal-based nonwoven fabrics had better physical/mechanical compatibility in the matrix (leading to better adherence/bonding) as these were more hydrophilic than ATW fibers. Further, long flax fibers (60 mm compared to short 6 mm ATW) may lead to stronger fiber anchorage and bonding with the matrix.
- Accelerated DW aging simulation on the ATW composites degraded the post-cracking properties, especially the toughness index by 50%, with respect to unaged conditions. This adverse effect could be compensated for nonwoven FRCMs when the matrix was treated with pozzolans (i.e., Silica Fume, SF). In this context, HTW composite replacing 30% of cement by SF lost only 20% of toughness, while the loss was 60% in PC.
- The flexural performance of nonwoven 100% flax and HTW FRCMs could be comparable to those woven FRCMs made of 100% PP, 100% AR glass, or vegetal fabrics. Indeed, the toughness (energy dissipation) and strain capacity of nonwoven FRCMs were more than twice that of glass counterparts. Nonetheless, nonwoven FRCMs had substantially lower stiffness and resistance (more than 70%) than synthetic p-aramid textile composites, thus unsuitable for structural retrofitting applications.

Thus, the results of this study proved that laminated cement composites reinforced with innovative nonwoven fabrics derived from textile waste could be alternative precast panels, mainly for architectural applications. Indeed, using costly and energy-intensive synthetic fiber textiles with high stiffness/tensile capacity (such as carbon or p-aramid) for many prefabricated construction components (especially under flexural mode), as well as strengthening the weak substrates (e.g., historical monuments) could be deemed unnecessary, considering sustainability and possible unexploited of those high capacities [87]. Future studies will be focused on the production of TW nonwoven FRCMs with a limited amount of PC (≤50%) in the ternary blended matrix (limestone calcined clay cement), as well as analyzing the microstructural behavior (including fiber-matrix interaction and pore structure, similar to the

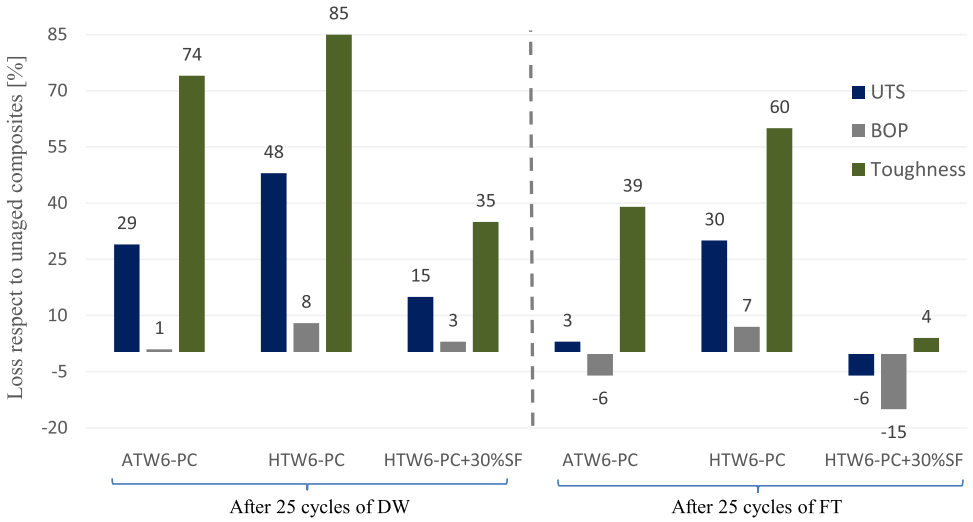

Fig. 8. Effect of accelerated cycling aging on the tensile properties of the nonwoven FRCMs (present study and [34]).

Table 6
Tensile properties of ATW shredded fibers at different conditions (coefficients of variance are in parentheses.).

Samples	Tensile strength [MPa]	Specific energy [J/m^2]	Modulus [GPa]
Unimmersed fiber	268.9 (18)	69.4 (37)	5.2 (34)
100%PC-5DW	219.6 (34)	59.4 (38)	3.8 (39)
90%PC-5DW	229.6. (17)	67.9 (39)	3.6 (22)
70%PC-5DW	246.5 (20)	75.2 (35)	3.4 (23)
50%PC-5DW	259.1 (19)	75.7 (33)	3.8 (31)
100%PC-10DW	206.3 (38)	40.1 (41)	3.9 (39)
90%PC-10DW	216.9 (13)	42.7 (40)	4.1 (24)
70%PC-10DW	219.1 (15)	45.1 (33)	4.2 (22)
50%PC-10DW	228.5 (21)	51.6 (41)	4.1 (22)

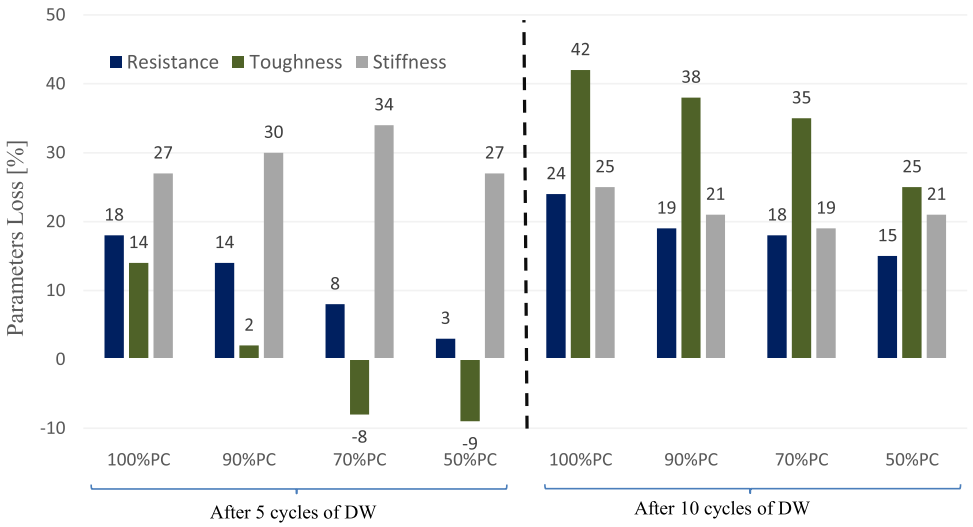

Fig. 9. Loss of tensile properties of the aged ATW fiber with respect to the unaged intact fiber.

methodology of [15]). Furthermore, the sustainability index of developed FRCM will be assessed by considering the economic-environmental-social aspects.

CRediT authorship contribution statement

Payam Sadrolodabaee: Writing – review & editing, Writing – original draft, Visualization, Validation, Software, Methodology, Investigation, Formal analysis, Data curation, Conceptualization. **Albert de la Fuente:** Writing – review & editing, Writing – original draft, Validation, Supervision, Resources, Methodology, Funding acquisition, Data curation. **Mònica Ardanuy:** Writing – review & editing, Writing – original draft, Supervision, Resources, Methodology, Funding acquisition, Conceptualization. **Josep Claramunt:** Writing – review & editing, Writing – original draft, Validation, Supervision, Methodology, Investigation, Funding acquisition, Formal analysis, Data curation, Conceptualization.

Declaration of Competing Interest

The authors declare that they have no known competing financial interests or personal relationships that could have appeared to influence the work reported in this paper.

Data Availability

Data will be made available on request.

Acknowledgments

The authors express their gratitude to the Agencia Estatal de Investigación, Spanish Ministry of Economy, Industry, and Competitiveness (Government of Spain) for the financial support received under the scope of the project RECYBUILDMAT (PID2019-108067RB-I00/AEI/10.13039/501100011033). Also, they acknowledge the funding of the research group TECTEX (2021 SGR 01056) from the *Department de Recerca i Universitats de la Generalitat de Catalunya*. The first author acknowledges the Banco Santander for the Research Scholarships (Postdoc-UPC 2022 Grant).

References

[1] "High energy performing buildings - Publications Office of the EU." [Online]. Available: ⟨https://publications.europa.eu/en/publication-detail/-/publication/d8e3702d-c782-11e8-9424-01aa75ed71a1/language-en/format-PDF/source-77709912⟩.
[2] C. Salzano, et al., Green building materials: mechanical performance and environmental sustainability, Mater. Sci. Forum vol. 1082 (Mar. 2023) 296–301, https://doi.org/10.4028/P-C090IH.
[3] I. Farina, I. Moccia, C. Salzano, N. Singh, P. Sadrolodabaee, F. Colangelo, Compressive and thermal properties of non-structural lightweight concrete containing industrial byproduct aggregates, Materials vol. 15 (11) (2022), https://doi.org/10.3390/ma15114029.
[4] F. de Andrade Salgado, F. de Andrade Silva, Recycled aggregates from construction and demolition waste towards an application on structural concrete: a review, J. Build. Eng. vol. 52 (Jul. 2022) 104452, https://doi.org/10.1016/J.JOBE.2022.104452.
[5] P. Sadrolodabaee, G. Di Rienzo, I. Farina, C. Salzano, N. Singh, F. Colangelo, Characterization of eco-friendly lightweight aggregate concretes incorporating industrial wastes, Key Eng. Mater. vol. 944 (Apr. 2023) 209–217, https://doi.org/10.4028/p-s77l3k.
[6] B. Lothenbach, K. Scrivener, R.D. Hooton, Supplementary cementitious materials, Cem. Concr. Res. vol. 41 (12) (Dec. 2011) 1244–1256, https://doi.org/10.1016/j.cemconres.2010.12.001.
[7] G. Liu, N. Tošić, A. de la Fuente, Recycling of macro-synthetic fiber-reinforced concrete and properties of new concretes with recycled aggregate and recovered fibers, vol. 13, no. 4, p. 2029, Feb. 2023, Appl. Sci. Vol. 13 (2023) 2029, https://doi.org/10.3390/APP13042029.
[8] P. Sadrolodabaee, J. Claramunt Blanes, M. Ardanuy Raso, and A. de la Fuente Antequera, Preliminary study on new micro textile waste fiber reinforced cement composite, ICBBM 2021: 4th International Conference on Bio-based Building Materials: Barcelona, Catalunya: June 16-18, 2021: proceedings, pp. 37–42, 2021, Accessed: Jul. 22, 2021. [Online]. Available: ⟨https://upcommons.upc.edu/handle/2117/348199⟩.
[9] P. Sadrolodabaee, Sustainability, durability and mechanical characterization of a new recycled textile-reinforced strain-hardening cementitious composite for building applications, Doctoral Thesis,UPC-BarcelonaTECH. [Online]. Available: ⟨https://www.tdx.cat/handle/10803/674796⟩.
[10] A.M. Brandt, Fibre reinforced cement-based (FRC) composites after over 40 years of development in building and civil engineering, Compos Struct. vol. 86 (1–3) (2008) 3–9, https://doi.org/10.1016/j.compstruct.2008.03.006.
[11] A.E. Alexander and A.P. Shashikala, Sustainability of Construction with Textile Reinforced Concrete- A State of the Art, in IOP Conference Series: Materials Science and Engineering, IOP Publishing Ltd, Oct. 2020. doi: 10.1088/1757-899X/936/1/012006.
[12] A. Morón, D. Ferrández, P. Saiz, C. Morón, Experimental study with cement mortars made with recycled concrete aggregate and reinforced with aramid fibers, Appl. Sci. 11 (17) (2021), https://doi.org/10.3390/app11177791.
[13] I. Curosu, M. Liebscher, V. Mechtcherine, C. Bellmann, S. Michel, Tensile behavior of high-strength strain-hardening cement-based composites (HS-SHCC) made with high-performance polyethylene, aramid and PBO fibers, Cem. Concr. Res 98 (2017) 71–81, https://doi.org/10.1016/j.cemconres.2017.04.004.
[14] N.P. Tran, C. Gunasekara, D.W. Law, S. Houshyar, S. Setunge, Utilization of recycled fabric-waste fibers in cementitious composite, J. Mater. Civ. Eng. 35 (1) (2023), https://doi.org/10.1061/(asce)mt.1943-5533.0004538.
[15] N.P. Tran, C. Gunasekara, D.W. Law, S. Houshyar, S. Setunge, Repurposing of blended fabric waste for sustainable cement-based composite: Mechanical and microstructural performance, Constr. Build. Mater. 362 (2023) 129785, https://doi.org/10.1016/J.CONBUILDMAT.2022.129785.
[16] M. Ardanuy, J. Claramunt, R.D. Toledo Filho, Cellulosic fiber reinforced cement-based composites: a review of recent research, Constr. Build. Mater. 79 (2015) 115–128, https://doi.org/10.1016/j.conbuildmat.2015.01.035.
[17] S. De Santis, F.G. Carozzi, G. de Felice, C. Poggi, Test methods for Textile Reinforced Mortar systems, Compos B Eng. vol. 127 (2017) 121–132, https://doi.org/10.1016/j.compositesb.2017.03.016.
[18] P. Sadrolodabaee, M. Ardanuy Raso, A. de la Fuente Antequera, and J. Claramunt Blanes, Cement composite panels reinforced with textile waste and flax nonwoven fabrics: flexural and accelerated aging performance, Booklet- ICBBM 2023 5th International Conference on Bio-based Building Materials, pp. 1–8, 2023, doi: 10.13039/501100011033).

[19] F.G. Carozzi *et al.*, Experimental investigation of tensile and bond properties of Carbon-FRCM composites for strengthening masonry elements, 2017, doi: 10.1016/j.compositesb.2017.06.018.

[20] M. Leone *et al.*, Glass fabric reinforced cementitious matrix: Tensile properties and bond performance on masonry substrate, 2017, doi: 10.1016/j.compositesb.2017.06.028.

[21] G. Piero Lignola et al., Performance assessment of basalt FRCM for retrofit applications on masonry, 2017, doi: 10.1016/j.compositesb.2017.05.003.

[22] C. Caggegi, et al., Experimental analysis on tensile and bond properties of PBO and aramid fabric reinforced cementitious matrix for strengthening masonry structures, Compos B Eng. vol. 127 (Oct. 2017) 175–195, https://doi.org/10.1016/j.compositesb.2017.05.048.

[23] M.E.A. Fidelis, F. de Andrade Silva, R.D. Toledo Filho, The influence of fiber treatment on the mechanical behavior of jute textile reinforced concrete, Key Eng. Mater. vol. 600 (Mar. 2014) 469–474, https://doi.org/10.4028/www.scientific.net/KEM.600.469.

[24] L. Mercedes, G. Castellazzi, E. Bernat-Maso, L. Gil, Matrix and fabric contribution on the tensile behaviour of fabric reinforced cementitious matrix composites, Constr. Build. Mater. vol. 363 (Jan. 2023), https://doi.org/10.1016/j.conbuildmat.2022.129693.

[25] H. Ahmad, M. Fan, Interfacial properties and structural performance of resin-coated natural fibre rebars within cementitious matrices, Cem. Concr. Compos vol. 87 (Mar. 2018) 44–52, https://doi.org/10.1016/J.CEMCONCOMP.2017.12.002.

[26] F. Micelli, M.A. Aiello, Residual tensile strength of dry and impregnated reinforcement fibres after exposure to alkaline environments, Compos B Eng. vol. 159 (Feb. 2019) 490–501, doi: 10.1016/J.COMPOSITESB.2017.03.005.

[27] J. Donnini, V. Corinaldesi, Mechanical characterization of different FRCM systems for structural reinforcement, Constr. Build. Mater. vol. 145 (Aug. 2017) 565–575, https://doi.org/10.1016/J.CONBUILDMAT.2017.04.051.

[28] M. Scheurer, et al., Current and future trends in textiles for concrete construction applications, Textiles vol. 3 (4) (Oct. 2023) 408–437, https://doi.org/10.3390/textiles3040025.

[29] R. Illampas, D.V. Oliveira, P.B. Lourenço, Design of strain-hardening natural TRM composites: current challenges and future research paths, Materials vol. 16 (13) (Jul. 2023), https://doi.org/10.3390/ma16134558.

[30] J. Claramunt, L.J. Fernández-Carrasco, H. Ventura, M. Ardanuy, Natural fiber nonwoven reinforced cement composites as sustainable materials for building envelopes, Constr. Build. Mater. vol. 115 (2016) 230–239, https://doi.org/10.1016/j.conbuildmat.2016.04.044.

[31] K.M.F. Hasan, P.G. Horváth, and T. Alpár, Potential fabric-reinforced composites: a comprehensive review, Journal of Materials Science, vol. 56, no. 26. Springer, pp. 14381–14415, Sep. 01, 2021. doi: 10.1007/s10853-021-06177-6.

[32] J. Claramunt, H. Ventura, L.J. Fernández-carrasco, M. Ardanuy, Tensile and flexural properties of cement composites reinforced with flax nonwoven fabrics, Materials (2017) 1–12, https://doi.org/10.3390/ma10020215.

[33] H. Ventura, M. Ardanuy, X. Capdevila, F. Cano, J.A. Tornero, Effects of needling parameters on some structural and physico-mechanical properties of needle-punched nonwovens, J. Text. Inst. vol. 105 (10) (2014) 1065–1075, https://doi.org/10.1080/00405000.2013.874628.

[34] P. Sadrolodabaee, J. Claramunt, M. Ardanuy, A. de la Fuente, Effect of accelerated aging and silica fume addition on the mechanical and microstructural properties of hybrid textile waste-flax fabric-reinforced cement composites, Cem. Concr. Compos vol. 135 (2023), https://doi.org/10.1016/j.cemconcomp.2022.104829.

[35] P. Sadrolodabaee, J. Claramunt, M. Ardanuy, A. de la Fuente, A textile waste fiber-reinforced cement composite: comparison between short random fiber and textile reinforcement, Materials 14 (13) (2021), https://doi.org/10.3390/ma14133742.

[36] P. Sadrolodabaee, J. Claramunt, M. Ardanuy, A.D.L. Fuente, Characterization of a textile waste nonwoven fabric reinforced cement composite for non-structural building components, Constr. Build. Mater. 276 (2021), https://doi.org/10.1016/j.conbuildmat.2020.122179.

[37] P. Sadrolodabaee, S.M.A. Hosseini, M. Ardunay, J. Claramunt, and A. de la Fuente, A New Sustainability Assessment Method for Façade Cladding Panels: A Case Study of Fiber/Textile Reinforced Cement Sheets, vol. 36. 2022. doi: 10.1007/978-3-030-83719-8_69.

[38] P. Sadrolodabaee, et al., Experimental characterization of comfort performance parameters and multi-criteria sustainability assessment of recycled textile-reinforced cement facade cladding, J. Clean. Prod. vol. 356 (2022), https://doi.org/10.1016/j.jclepro.2022.131900.

[39] N.P. Tran, C. Gunasekara, D.W. Law, S. Houshyar, S. Setunge, A. Cwirzen, Comprehensive review on sustainable fiber reinforced concrete incorporating recycled textile waste, vol. 0, no. 0, J. Sustain Cem. Based Mater. (2021) 1–22, https://doi.org/10.1080/21650373.2021.1875273.

[40] J.M. Hawley, Textile recycling: A systems perspective, *Recycling in textiles*, 2006, Accessed: Apr. 17, 2019. [Online]. Available: ⟨http://krex.k-state.edu/dspace/handle/2097/595⟩.

[41] Textiles - EuRIC." Accessed: Apr. 30, 2023. [Online]. Available: ⟨https://euric-aisbl.eu/what-we-recycle/textiles⟩.

[42] A. Beton *et al.*, Environmental Improvement Potential of textiles (IMPRO Textiles), Report EUR 26316 EN, 2014, doi: 10.2791/52624.

[43] F. Nerilli and B. Ferracuti, A tension stiffening model for FRCM reinforcements calibrated by means of an extended database, 2022, doi: 10.17632/4zg9.

[44] B. Mobasher, V. Dey, Z. Cohen, A. Peled, Correlation of constitutive response of hybrid textile reinforced concrete from tensile and flexural tests, Cem. Concr. Compos vol. 53 (2014) 148–161, https://doi.org/10.1016/j.cemconcomp.2014.06.004.

[45] S. De Santis, G. De Felice, Tensile behaviour of mortar-based composites for externally bonded reinforcement systems, *Compos B Eng.* vol. 68 (2015) 401–413, https://doi.org/10.1016/j.compositesb.2014.09.011.

[46] A. Peled, Z. Cohen, Y. Pasder, A. Roye, T. Gries, Influences of textile characteristics on the tensile properties of warp knitted cement based composites, Cem. Concr. Compos vol. 30 (3) (Mar. 2008) 174–183, https://doi.org/10.1016/j.cemconcomp.2007.09.001.

[47] S. Paul, R. Gettu, D. Naidu Arnepalli, R. Samanthula, Experimental evaluation of the durability of glass Textile-Reinforced concrete, Constr. Build. Mater. vol. 406 (Nov. 2023), https://doi.org/10.1016/j.conbuildmat.2023.133390.

[48] O.A. Cevallos, R.S. Olivito, Effects of fabric parameters on the tensile behaviour of sustainable cementitious composites, Compos B Eng. vol. 69 (2015) 256–266, https://doi.org/10.1016/j.compositesb.2014.10.004.

[49] F. de A. Silva, B. Mobasher, R.D.T. Filho, Cracking mechanisms in durable sisal fiber reinforced cement composites, Cem. Concr. Compos vol. 31 (10) (2009) 721–730, https://doi.org/10.1016/j.cemconcomp.2009.07.004.

[50] G. Ferrara, M. Pepe, E. Martinelli, R.D. Tolêdo Filho, Tensile behavior of flax textile reinforced lime-mortar: influence of reinforcement amount and textile impregnation, Cem. Concr. Compos 119 (2021) 103984, https://doi.org/10.1016/j.cemconcomp.2021.103984.

[51] M. Alma'aitah, B. Ghiassi, Development of cost-effective low carbon hybrid textile reinforced concrete for structural or repair applications, Constr. Build. Mater. 341 (2022), https://doi.org/10.1016/j.conbuildmat.2022.127858.

[52] F. Majstorović, V. Sebera, M. Mrak, S. Dolenec, M. Wolf, L. Marrot, Impact of metakaolin on mechanical performance of flax textile-reinforced cement-based composites, Cem. Concr. Compos 126 (2022) 104367, https://doi.org/10.1016/J.CEMCONCOMP.2021.104367.

[53] R.D. Toledo Filho, F. de, A. Silva, E.M.R. Fairbairn, J. de A.M. Filho, Durability of compression molded sisal fiber reinforced mortar laminates, Constr. Build. Mater. 23 (6) (2009) 2409–2420, https://doi.org/10.1016/J.CONBUILDMAT.2008.10.012.

[54] "D6272 Standard Test Method for Flexural Properties of Unreinforced and Reinforced Plastics and Electrical Insulating Materials by Four-Point Bending."

[55] RILEM Technical Committee 232-TDT (Wolfgang Brameshuber) et al., Recommendation of RILEM TC 232-TDT: test methods and design of textile reinforced concrete: Uniaxial tensile test: test method to determine the load bearing behavior of tensile specimens made of textile reinforced concrete, Materials and Structures/Materiaux et Constructions, vol. 49, no. 12, pp. 4923–4927, May 2016, doi: 10.1617/S11527-016-0839-Z/FIGURES/3.

[56] N. Azimi, A. Dalalbashi, D.V. Oliveira, B. Ghiassi, P.B. Lourenço, Tensile behavior of textile-reinforced mortar: influence of test setup and layer arrangement, Constr. Build. Mater. 394 (2023), https://doi.org/10.1016/j.conbuildmat.2023.132185.

[57] S.K. John, Y. Nadir, N.K. Safwan, P.C. Swaliha, K. Sreelakshmi, V.A. Nambiar, Tensile and bond behaviour of basalt and glass textile reinforced geopolymer composites, J. Build. Eng. 72 (2023) 106540, https://doi.org/10.1016/J.JOBE.2023.106540.

[58] M. Alma'aitah, B. Ghiassi, Development of Low Carbon Textile Reinforced Concrete from Composite Cements, in: RILEM Bookseries, vol. 44, Springer Science and Business Media B.V, 2023, pp. 240–249, https://doi.org/10.1007/978-3-031-33187-9_23.

[59] M. Ramirez, J. Claramunt, H. Ventura, M. Ardanuy, Evaluation of the mechanical performance and durability of binary blended CAC-MK/natural fiber composites (vol. In progres), Constr. Build. Mater. (2019), https://doi.org/10.1016/j.conbuildmat.2020.118919.

[60] F.D. Tolêdo Romildo D, K. Ghavami, G.L. England, K. Scrivener, Development of vegetable fibre-mortar composites of improved durability, Cem. Concr. Compos 25 (2) (2003) 185–196, https://doi.org/10.1016/S0958-9465(02)00018-5.
[61] P. Sadrolodabaee, J. Claramunt, M. Ardanuy, and A. de la Fuente, Durability of Eco-Friendly Strain-Hardening Cementitious Composite incorporating Recycled Textile Waste Fiber and Silica Fume, in fib Symposium, 14th fib PhD Symposium in Civil Engineering, 2022 Rome: fib. The International Federation for Structural Concrete, 2022, pp. 321–328. [Online]. Available: ⟨http://hdl.handle.net/2117/386845⟩.
[62] AC434, AC434: Acceptance Criteria for Masonry and Concrete Strengthening Using Fiber-reinforced Cementitious Matrix (FRCM) Composite Systems, vol. AC434, 2013.
[63] G. de Felice, et al., Recommendation of RILEM Technical Committee 250-CSM: test method for Textile Reinforced Mortar to substrate bond characterization, Mater. Struct. /Mater. Et. Constr. 51 (4) (2018) 1–9, doi: 10.1617/S11527-018-1216-X/FIGURES/3.
[64] F. ACI Committee 549, Guide to Design and Construction of Externally Bonded Fabric-Reinforced Cementitious Matrix (FRCM) Systems for Repair and Strengthening Concrete and Masonry Structures, vol. ACI 549-.4R-13, p. 69, 2013.
[65] A. Abbass, P.B. Lourenço, D.V. Oliveira, The use of natural fibers in repairing and strengthening of cultural heritage buildings, Mater. Today Proc. 31 (2020) S321–S328, https://doi.org/10.1016/J.MATPR.2020.02.206.
[66] H. Ventura, M.D. Álvarez, L. Gonzalez-Lopez, J. Claramunt, M. Ardanuy, Cement composite plates reinforced with nonwoven fabrics from technical textile waste fibres: mechanical and environmental assessment, J. Clean. Prod. 372 (2022) 133652, https://doi.org/10.1016/J.JCLEPRO.2022.133652.
[67] M. De Munck, et al., Durability of sandwich beams with textile reinforced cementitious composite faces, Constr. Build. Mater. 229 (2019), https://doi.org/10.1016/j.conbuildmat.2019.116832.
[68] "BS EN 12467:2012+A2:2018 Fibre-cement flat sheets. Product specification and test methods - European Standards." Accessed: Sep. 09, 2022. [Online]. Available: ⟨https://www.en-standard.eu/bs-en-12467-2012-a2-2018-fibre-cement-flat-sheets-product-specification-and-test-methods/⟩.
[69] T. R.-R. R. for the T. and U. of and undefined 1994, TFR 1 Test for the determination of modulus of rupture and limit of proportionality of thin fibre reinforced cement sections, 1984, rilem.net.
[70] RILEM, The determinarion of energy absortion in flexure of thin fibre reinforced cement sections, Mater Struct, vol. 17, no. No. 102, pp. 171–173, 1984.
[71] "ASTM-C1557-20-Standard test method for tensile strength and Young's modulus of fibers.".
[72] R.D. Tolêdo Filho, K. Scrivener, G.L. England, K. Ghavami, Durability of alkali-sensitive sisal and coconut fibres in cement mortar composites, Cem. Concr. Compos 22 (2) (2000) 127–143, https://doi.org/10.1016/S0958-9465(99)00039-6.
[73] P. Sadrolodabaee, J. Claramunt, M. Ardanuy, A. de la Fuente, Mechanical and durability characterization of a new textile waste micro-fiber reinforced cement composite for building applications, Case Stud. Constr. Mater. 14 (2021), https://doi.org/10.1016/j.cscm.2021.e00492.
[74] J. Claramunt, M. Ardanuy, J.A. García-Hortal, R.D.T. Filho, The hornification of vegetable fibers to improve the durability of cement mortar composites, Cem. Concr. Compos 33 (5) (2011) 586–595, https://doi.org/10.1016/j.cemconcomp.2011.03.003.
[75] B. Mobasher, Mechanics of fiber and textile reinforced cement composites. 2011. doi: 10.1201/b11181.
[76] A.R. Mahpour, et al., Serviceability parameters and social sustainability assessment of flax fabric reinforced lime-based drywall interior panels, J. Build. Eng. 76 (2023), https://doi.org/10.1016/j.jobe.2023.107406.
[77] F.D.A. Silva, R.D.T. Filho, J.D.A.M. Filho, E.D.M.R. Fairbairn, Physical and mechanical properties of durable sisal fiber–cement composites, Constr. Build. Mater. 24 (5) (2010) 777–785, https://doi.org/10.1016/j.conbuildmat.2009.10.030.
[78] B.J. Mohr, H. Nanko, K.E. Kurtis, Durability of kraft pulp fiber–cement composites to wet/dry cycling, Cem. Concr. Compos 27 (4) (2005) 435–448, https://doi.org/10.1016/J.CEMCONCOMP.2004.07.006.
[79] S. Yin, L. Jing, M. Yin, B. Wang, Mechanical properties of textile reinforced concrete under chloride wet-dry and freeze-thaw cycle environments, Cem. Concr. Compos 96 (2019) 118–127, https://doi.org/10.1016/j.cemconcomp.2018.11.020.
[80] P. Larrinaga, C. Chastre, J.T. San-José, L. Garmendia, Non-linear analytical model of composites based on basalt textile reinforced mortar under uniaxial tension, Compos B Eng. 55 (2013) 518–527, https://doi.org/10.1016/J.COMPOSITESB.2013.06.043.
[81] S. Paul, R. Gettu, Engineering the tensile response of glass textile reinforced concrete for thin elements, Sustainability vol. 15 (19) (2023) 14502, https://doi.org/10.3390/su151914502.
[82] M. Saidi, A. Gabor, Iterative analytical modelling of the global behaviour of textile-reinforced cementitious matrix composites subjected to tensile loading, Constr. Build. Mater. 263 (2020) 120130, https://doi.org/10.1016/j.conbuildmat.2020.120130.
[83] J. Zhang, et al., Study of aramid and carbon fibers on the tensile properties of early strength cement mortar, IOP Conf. Ser. Earth Environ. Sci. 267 (3) (2019) 032009, https://doi.org/10.1088/1755-1315/267/3/032009.
[84] S.R. Ferreira, M. Pepe, E. Martinelli, F. de Andrade Silva, R.D. Toledo Filho, Influence of natural fibers characteristics on the interface mechanics with cement based matrices, Compos B Eng. 140 (2018) 183–196, https://doi.org/10.1016/j.compositesb.2017.12.016.
[85] M.E.A. Fidelis, R.D. Toledo Filho, F. de Andrade Silva, B. Mobasher, S. Müller, V. Mechtcherine, Interface characteristics of jute fiber systems in a cementitious matrix, Cem. Concr. Res 116 (2019) 252–265, https://doi.org/10.1016/j.cemconres.2018.12.002.
[86] V. Da Costa Correia, S.F. Santos, G. Mármol, A. Aprigio, S. Curvelo, and H. Savastano, Potential of bamboo organosolv pulp as a reinforcing element in fiber-cement materials, 2014, doi: 10.1016/j.conbuildmat.2014.09.005.
[87] P. Sadrolodabaee, M. Ardanuy, A. de la Fuente, J. Claramunt, Valorization of Textile Waste in Laminated Fabric Reinforced Cementitious Matrix Plates: Tensile and Durability Characterization, in: N. Banthia, S. Soleimani-Dashtaki, S. Mindess (Eds.), Smart & Sustainable Infrastructure: Building a Greener Tomorrow, 2023RILEM Bookseries, 48, Springer, Cham, ISSSI, 2024, https://doi.org/10.1007/978-3-031-53389-1_81.